



MINISTRY OF AVIATION  
 AERONAUTICAL RESEARCH COUNCIL  
 CURRENT PAPERS

An Investigation into the Effects of Ground Proximity  
 on Twin Coaxial Annular Jets, using Hot and Cold Air

By

By *R.V. Barrett and J.C. Tipping*

**DERA Information Centre**  
 No. 1 Building  
 DERA  
 Clapham  
 Bedford  
 MK41 6AE  
 Tel. 01234 225099  
 Fax: 01234 225011  
 ICE: Hurry Pat

Please return this publication to the Information  
 Centre, or request a renewal, by the date last  
 stamped below.

NAME	RETURN BY
D LONNERS S + S	14 APR 1998 2013198

**DERA**  
 Information Resources

An Investigation into the Effects of Ground Proximity  
on Twin Coaxial Annular Jets, using Hot and Cold Air

- By -

R. V. Barrett and J. C. Tipping

---

Communicated by Prof. A. R. Collar

---

June, 1960

SUMMARY

Changes of the conditions in a jet, issuing from a twin coaxial annular nozzle system, due to proximity of a ground board perpendicular to the flow, were studied. Provision was made for heating the inner annular jet to simulate a projected type of lifting engine for V.T.O.L. aircraft.

The principal measurements made were of thrust and temperature distribution in the jet, but extensive flow visualisation was also carried out.

The jet configuration was found to give a thrust 5% lower than the theoretical value when in free air, and an augmentation of thrust for close proximity of the ground board. Both these effects were shown to be mainly due to the magnitude of the pressures on the nozzle base areas. Heating the inner jet did not produce any noticeable change in the thrust augmentation effect.

The temperature distribution in the jet was found to undergo considerable changes as the distance of the ground board from the nozzle was decreased.

An attempt was made to correlate the thrust and temperature measurements with the observed flow.

---

List/

List of Contents

	<u>Pages</u>
List of Symbols .. .. .	3
1. Introduction .. .. .	4
2. Apparatus .. .. .	4
2.1 Nozzles and plenum chambers .. .. .	4
2.1.1 Plenum chambers .. .. .	5
2.1.2 Nozzles .. .. .	5
2.2 Thrust balance .. .. .	5
2.3 Ground board .. .. .	6
2.4 Air heater .. .. .	6
2.5 Thermocouple probe .. .. .	6
2.6 Pressure probes .. .. .	6
2.7 Traversing rig .. .. .	6
2.8 Flow meters .. .. .	6
2.9 Schlieren apparatus .. .. .	6
3. Experimental Procedure .. .. .	6
3.1 Balance measurements .. .. .	7
3.2 Pressure measurements .. .. .	7
3.2.1 Nozzle and plenum chamber pressures .. .. .	7
3.2.2 Ground board pressures .. .. .	7
3.2.3 Pressure traverses .. .. .	7
3.3 Temperature measurements .. .. .	7
3.4 Flow visualisation .. .. .	7
3.4.1 Schlieren photography .. .. .	7
3.4.2 Temperature indicating paints .. .. .	8
3.4.3 Oil film .. .. .	8
3.4.4 Wool tuft probe .. .. .	8
4. Theory .. .. .	8
4.1 Thrust coefficients .. .. .	8
4.2 Theoretical thrust .. .. .	8
4.3 Ground board pressure integration .. .. .	9
4.4 Ground board proximity parameter .. .. .	9
4.5 Jet velocity .. .. .	9
4.6 Jet total heat .. .. .	9
5. Results and Discussion .. .. .	10
5.1 Thrust measurements .. .. .	10
5.2 Temperature measurements .. .. .	10
5.3 Flow visualisation .. .. .	11
5.3.1 Schlieren photographs and shadowgraph traces .. .. .	11
5.3.2 Temperature indicating paints .. .. .	12
5.3.3 Wool tuft probe .. .. .	12
5.3.4 Oil film .. .. .	12
5.4 Jet velocity and total heat (for the jet in free air) .. .. .	12
6. Conclusions .. .. .	13
References .. .. .	14
Appendix - Design and Development of the Air Heater .. .. .	15
Figures	

List of Symbols

A Cross-sectional area ( $\text{in.}^2$ )

Suffices

i Inner nozzle exit

o Outer nozzle exit

D Nozzle reference diameter (2.0 in.)

H Distance from nozzle exit to ground board (in.)

h Vertical distances from nozzle exit to a point in the flow (in.)

r Radial distance from centre of ground board (in.)

P Pressures ( $\text{lb/ft}^2$ ). Absolute

Suffices

a Atmospheric pressure

g Pressure on the ground board

i Inner nozzle static pressure at exit

o Outer nozzle static pressure at exit

T Total pressure at a point in the jet

s Static pressure at a point in the jet

T Thrust (lb wt)

Suffices

B Thrust measured by balance

G Thrust calculated from ground board pressure integration

N Nozzle base pressure thrust term

T Theoretical thrust

V Jet velocity (ft/sec)

Suffices

i At inner nozzle exit

o At outer nozzle exit

- $\rho_0$  Standard density at sea-level 0.00238 slugs/cu ft
- $\rho_t$  Density in the jet at a temperature  $t^\circ\text{C}$  (slugs/cu ft)
- $C_T$  Thrust coefficient  $C_T = \left( \frac{T_B}{T_T} \right)$
- $C_T^*$  Thrust coefficient  $C_T^* = \left( \frac{T_g}{T_T} \right)$
- $H/D$  Ground proximity parameter
- $Q$  Total heat above ambient temperature passing a reference section in the jet (B tu/sec)
- $C_p$  Specific heat at constant pressure (0.432 B tu/lb/ $^\circ\text{C}$ )
- $g$  Acceleration due to gravity (32.2 ft/sec<sup>2</sup>).

## 1. Introduction

This report is concerned with a problem relating to vertical take-off aircraft of a type employing engines solely for lifting purposes. A proposed design for such an engine is shown in Fig. 1; it is in effect a low compression ratio ducted fan engine. Modern engine development indicates that thrust:weight ratios in the order of 14:1 are to be expected, compared with thrust:weight ratios of 6:1 for the most powerful ducted fan engines at present available.

Specialized lifting engines are particularly suited to large multi-engined V.T.O.L. aircraft. Under normal cruising conditions the thrust required for such an aircraft is never more than 10% of its weight, thus the lifting engines would be carried as dead weight for most of the flight. Despite this fact their light weight and high thrust would make this type of aircraft an economic possibility. Another application of these engines is for a low-speed wingless vehicle with a high load-carrying capacity, capable of performing similar work to the helicopter.

For all types of V.T.O.L. aircraft the effect of ground proximity on the thrust available for lifting is of great importance. The problem of an annular jet impinging on the ground was first studied, by von Glahn<sup>1</sup> and later by Childes and Fisher<sup>2</sup>, using a cold jet. The present investigation is an extension of this work, using conditions nearer to those of the proposed lifting engine shown in Fig. 1, with twin annular nozzles and a hot inner jet.

A study has been made of the effect of ground proximity on the thrust and also on the mixing of the hot and cold jets. No theoretical approach to the mixing problem has been attempted. All mixing theory to date has dealt with simpler cases such as a circular nozzle discharging into a moving stream<sup>3,4</sup>. The most closely related experimental work to the present investigation was by Burley and Bryant<sup>5</sup>. This was an investigation into the mixing of the hot and cold jets in the tailpipe of a simulated bypass engine.

## 2. Apparatus

### 2.1 Nozzles and plenum chambers

The nozzle and plenum chamber assembly is shown in Figs. 3 and 4. The air to the hot and cold jets was supplied through two completely separate systems. The hot air was passed through a plenum chamber to the inner annular nozzle, while the cold air passed through an outer plenum chamber to the second annular nozzle, coaxial with the first.

The plenum chambers and nozzles will be described separately.

### 2.1.1 Plenum chambers

The inner plenum chamber consisted of a 5 in. diameter steel cylinder of length 10 in. The hot air entered this through a  $\frac{3}{4}$  in. bore pipe. Inside the plenum chamber the air was first spread by means of a sheet metal cone, perforated to reduce the formation of eddy vortices. The flow was subsequently "straightened" by two wire gauzes.

Cold air was supplied to the outer plenum chamber through twin inlets in the top plate. The air was spread by a perforated inverted cone and then passed down an annular chamber containing three wire gauzes to "straighten" the flow. This chamber had an outer diameter of 9 in. and a width of 1 in. The space between the inner and outer plenum chamber was filled with fibreglass lagging to reduce the heating of the cold air to a minimum.

Four bolts bearing on the lower flange of the inner plenum chamber were provided to facilitate lining-up the complete assembly. Static pressure tappings were taken from the lower ends of both plenum chambers. The method of mounting the plenum chambers on to the balance arm is shown in Fig. 3.

### 2.1.2 Nozzles

The coaxial annular nozzles were formed from two fibreglass shells and a streamlined centre body, as shown in Fig. 4.

The brass centre body was made in three sections and was mounted in the nozzle by four thin steel vanes. Five pressure tappings were provided on a diameter of the centre body base plate. Due to high temperatures involved these tappings were connected with stainless steel tubes which passed directly out through the inner fibreglass shell. It was found necessary to use a special resin, (Marco S.B. 28.D.)<sup>8</sup>, for bonding the inner surface of the inner fibreglass shell as normal resins were not capable of withstanding the high temperatures required for the tests. This special resin could withstand temperatures of 200°C for an indefinite period, and proved satisfactory throughout the tests. The inner shell was built up with asbestos string soaked in resin, and completed with layers of fibreglass cloth. The smooth outer surface was obtained by machining.

The two pressure tappings on the annular base, and the inner nozzle static pressure tappings, were connected with stainless steel tubes moulded into the inner shell. The dimensions of the nozzle outlets are given in Fig. 8.

## 2.2 Thrust balance (Fig. 2)

The nozzle assembly was mounted on one end of a simple beam balance supported on a cross-spring fulcrum. The problem of supplying air to the nozzle without affecting the reading of the balance was overcome by delivering both the hot and cold air through rubber hoses at right angles to the nozzle thrust line. As the balance was necessarily a null point device the only effect of the hoses was to provide damping. The weight of the nozzle assembly was counterbalanced by a concentrated mass at the

### 2.3 Ground board

The 2 ft square ground board was provided with 21 pressure tapplings along a radial line and 4 check pressure tapplings on the opposite radius. It was mounted normal to the jet thrust line and its height beneath the nozzle was adjustable. To prevent warping at the high temperatures involved the ground board was constructed from  $\frac{3}{4}$  in. "chipboard", which was topped with a 16 gauge steel plate.

### 2.4 Air heater

The air heater is shown in Figs. 5 and 7. The gas was induced into the heater by a high velocity jet of air. The gas and air were then mixed and burnt in a narrow circular combustion chamber. Ignition of the mixture was by a miniature glow plug fitted into the mixing tube. Hot products of combustion passed down an inner tube and then mixed with the main air supply which was brought in separately. The gas and injector air supplies were controlled by valves so that the correct stoichiometric mixture could be maintained in the combustion chamber. For the mass flow used, the air temperature could be kept constant at any value between 100°C and 200°C. A thermometer was incorporated into the heater tube to provide a reference temperature.

A full account of the design and development of the heater is given in the Appendix.

### 2.5 Thermocouple probe

The construction of the thermocouple is shown in Fig. 9; its two junction leads were of chromel and alumel alloys. The probe was connected to a potentiometer circuit, incorporating a 'standard cell', enabling temperatures to be measured to within 1.0°C.

### 2.6 Pressure probes

Small total and static pressure probes were constructed for traversing the jet.

### 2.7 Traversing rig

The traversing rig incorporated two calibrated scales for vertical and horizontal movement. The thermocouple probe and the two pressure probes were interchangeable in this rig.

### 2.8 Flow meters

The mass flow of the cold air to the outer nozzle was measured by an orifice plate meter in the supply line. The main air supply to the heater was measured by a "three-quarter radius pitot tube flow meter"<sup>6</sup>. The mass flow of secondary air through the injector nozzle was calibrated against the position of the turn screw on the inlet valve. For stoichiometric conditions the mass flow of gas could be found knowing the mass flow of injector air. Calibration of the meters was checked by total head traverses at the nozzle efflux.

### 2.9 Schlieren apparatus

A normal double mirror system was employed with a Mazdalux mercury vapour lamp source.

## 3. Experimental Procedure

Throughout the tests a constant mass flow ratio between the jets was used, the ratio being:-

Outer/

$$\frac{\text{Outer jet mass flow}}{\text{Inner jet mass flow}} = \frac{2.5}{1}$$

The majority of tests were conducted at mass flows of 4 lb/min and 10 lb/min for the inner and outer jets respectively. One series of tests was conducted using twice these mass flows. Measurements were taken with the inner jet hot and outer jet cold and with both jets cold. In the figures these are referred to as H/C, C/C runs while in the text they are referred to as hot runs or cold runs. The reference temperature for the hot jet was 160°C throughout the tests.

### 3.1 Balance measurements

Direct thrust measurements were obtained from the beam balance. Using the mass flows stated above, with the centre jet hot and the outer jet cold, the thrust was measured for the nozzle in free air and at ground board positions of H/D ranging from 4.0 to 0.25. The procedure was repeated with both jets cold, for the same mass flow, and also for double the mass flow.

### 3.2 Pressure measurements

#### 3.2.1 Nozzle and plenum chamber pressures

Static pressures in the plenum chambers and at the nozzle exits were recorded. Pressures on the base of the nozzle were also recorded, at the tapping positions shown in Fig. 8. These pressures were measured for the tests using the lower total mass flow of 14 lb/min; all other conditions being the same as in Section 3.1.

#### 3.2.2 Ground board pressures

The pressure distribution over the ground boards was recorded using a multi-tube manometer for all the test conditions previously stated. Values of the thrust were obtained by integrating these pressures over the area of the ground board.

#### 3.2.3 Pressure traverses

The jet was traversed with total and static pressure probes at intervals from the nozzle exit. Because the proximity of the ground board affected the direction of the flow, these measurements were only taken for the jet in free air.

### 3.3 Temperature measurements

Traverses were made with a thermocouple probe at close intervals down the jet for a heater reference temperature of 160°C ± 1°C. These tests were conducted for the jet in free air, and values of H/D ranging from 2.0 to 0.25, using the lower mass flow of 14 lb/min.

### 3.4 Flow visualisation

#### 3.4.1 Schlieren photography



Kodak P.1600 plates were used with a shutter speed of  $\frac{1}{200}$  sec. Shadowgraphs of the flow were also obtained by tracing the image thrown on a screen placed about 3 ft behind the nozzle.

### 3.4.2 Temperature indicating paints

A set of 'Thermindex' temperature indicating paints<sup>9</sup> were used in an attempt to obtain temperature contours in the jet and on the ground board. The paints were designed to give a clear colour change at a set temperature, after having been exposed to this temperature for a standard calibration time of 10 minutes.

The following paints were tried:-

<u>Ref. No.</u>	<u>Colour Change</u>	<u>Transition Temp.</u>
G.87	Pink - Lavender	80°C
E.102	Pink - Blue Violet	115°C
G.G.55	Mauve Pink - Bright Blue	140°C
E.91	Dull Blue - Green	145°C

These paints were sprayed onto thin aluminium splitter plates which were then left in the jet for 10 minutes. The splitter plates were necessarily thin to reduce conduction of heat through the metal to the colder parts of the jet, as conduction of this type tended to spread the contours beyond their correct boundaries.

Ground temperature contours were obtained by placing similarly prepared plates on top of the ground board.

### 3.4.3 Oil film

The jet flow was also studied by the oil film technique. The oil film mixture consisted of titanium oxide powder suspended in paraffin oil, together with a small proportion of oleic acid. This mixture was used on splitter plates in a vertical diametral plane of the jet, for various heights of the ground board.

### 3.4.4 Wool tuft probe

The flow in the jet was investigated, using a wool tuft probe, for various heights of the ground board.

## 4. Theory

### 4.1 Thrust coefficients

The following non-dimensional thrust coefficients were used:-

$$C_T = \frac{\text{Balance, measurement of thrust}}{\text{Theoretical thrust}} = \frac{T_B}{T_T}$$

$$C_T^* = \frac{\text{Thrust derived from ground pressure integration}}{\text{Theoretical thrust}} = \frac{T_G}{T_T}$$

### 4.2 Theoretical thrust

This was derived by considering momentum changes in the jet and the pressure force on the jet efflux areas. Compressibility effects were negligible at the jet velocities used.

The theoretical thrust  $T_T$  is given by:-

$$T_T = m_i V_{i1} + m_o V_o + \left( \frac{A_i}{144} \right) (P_i - P_a) + \left( \frac{A_o}{144} \right) (P_o - P_a)$$

where  $T_T$  is the thrust in lb wt.

#### 4.3 Ground board pressure integration

The reaction force  $T_G$  on the ground board is theoretically equal to the measured thrust  $T_B$ , providing the ground board is of sufficient size.

$$T_G \text{ is given by } 2\pi \int_0^{\infty} (P_g - P_a) r \cdot dr. \text{ lb wt.}$$

The integral was evaluated by plotting  $(P_g - P_a)r$  against 'r' and calculating the areas under the curves.

#### 4.4 Ground board proximity parameter

The distance of the ground board from the nozzle was defined by the non-dimensional parameter  $H/D$ . The nozzle reference diameter  $D$  was taken as the central diameter of the outer annular jet for convenience, as this was exactly 2.0 in.

#### 4.5 Jet velocity

The jet velocity,  $V$ , at a point in the flow was calculated as follows.

$$V = \sqrt{\frac{2(P_T - P_S)}{\rho_t}} \text{ ft/sec}$$

where  $\rho_t$  is given by  $\rho_t = \rho_o \left( \frac{288}{273 + t} \right)$  as density changes due to changes in pressure were assumed to be negligible.

#### 4.6 Jet total heat

The total heat,  $Q$ , (above ambient temperature) passing a reference section per second was calculated as indicated below.

Heat passing through a small element of area  $\delta A$  is

$$\delta Q = \rho_t \cdot V \cdot \delta A \cdot C_p \cdot (t - t_a) \cdot g. \text{ B.t.u./sec.}$$

Hence the total heat passing per second is given by

$$Q = 2\pi \cdot g \cdot C_p \int_0^{\infty} \rho_t \cdot V \cdot (t - t_a) \cdot r \cdot dr. \text{ B.t.u./sec.}$$

## 5. Results and Discussion

### 5.1 Thrust measurements

The variation of thrust coefficient  $C_T$ , with ground proximity parameter  $H/D$ , is shown in Fig. 10 for both 'hot runs' and 'cold runs', with a constant mass flow of 14 lb/min. The two curves were identical, showing that heating the inner jet had no effect on the thrust augmentation. It is shown from the figure that in free air the thrust was only 95% of the

theoretical value. Thrust augmentation began at  $\frac{H}{D} = 2.0$ , and at  $\frac{H}{D} = 1.25$  the thrust had reached the theoretical value. At smaller values of  $\frac{H}{D}$  the thrust became greater than theoretical, and at  $\frac{H}{D} = 1.0$  and  $0.5$  it was respectively 10% and 30% greater than the free air value.

Thrust variations from the theoretical value were considered to be mainly due to pressure changes on the centre-body and annular bases of the nozzle. Fig. 11 shows these pressures relative to atmospheric pressure, plotted against the ground proximity parameter. These curves were similar for the hot and cold runs. They show suction under both bases for the jet in free air, and pressures for small values of the ground proximity parameter.

By integrating the base pressures over their respective areas and adding the force term obtained to the theoretical thrust, curves were obtained which were compared directly with the balance measurements of thrust, (Figs. 12 and 13). Reasonable agreement was shown for both hot and cold runs thus verifying the relation between thrust changes and base pressures. As the number of pressureappings on the bases was small, the pressure integrations could only be approximate, and even better agreement might have been shown if the exact pressure profiles had been known.

A practical engine with this jet configuration would require the thrust loss in free air to be reduced to a minimum. This could possibly be achieved by streamlining the bases, or angling the jets inwards. No study was made of this aspect, but Fisher and Childes<sup>2</sup>, showed that for a single annular jet, streamlining the centre-body had a beneficial effect.

In order to show whether increasing the jet velocities altered the thrust augmentation profile, a cold run at twice the normal mass flow in each jet was carried out. Fig. 14 shows that there was very little change in the profile at the higher jet velocities.

The pressure distributions over the ground board for the complete range of ground board heights are shown in Figs. 24 and 25. These were integrated over the area of the ground board: the thrust curves obtained are shown in Fig. 15.

The curves did not give good agreement with those obtained from the balance measurements, except at values of the ground proximity parameter less than 0.5. No single reason could be found for the discrepancy, but it was thought that asymmetry of the jet was partly responsible. A study of asymmetry at ground board level was made with an airflow meter. The results indicated that slight asymmetry was present, the direction and magnitude of which, changed with the position of the ground board.

### 5.2 Temperature measurements

The temperature distribution in the jet for free air, and values of the ground proximity parameter from 2.0 to 0.25 are shown in Figs. 16 to 22. Each figure shows a selection of the traverses taken through the jet, and the isothermals derived therefrom. In each case the jet efflux temperature was 160°C.

A marked similarity was apparent between the isothermal shapes of the jet in free air, and for values of  $H/D$  of 2.0 and 1.5. The only differences were a 'widening' of the isothermals near the ground, (which can be seen by referring to the 70°C isothermal in each figure), and a reduction of temperature under the centre-body at  $\frac{H}{D} = 1.5$ . This latter effect was not apparent at  $\frac{H}{D} = 2.0$ , but became most marked at  $\frac{H}{D} = 1.0$ . On decreasing the ground proximity parameter still further, the temperature again rose under the centre-body until at  $\frac{H}{D} = 0.25$  the whole central area was above 150°C.

For the jet in free air, and for the larger values of the ground proximity parameter, the isothermals were grouped into two regions of high-temperature gradient, separated by a large area of fairly constant temperature between 60°C and 80°C. The grouping of the isothermals changed at  $\frac{H}{D} = 1.0$  to one large region of high-temperature gradient at the outside of the jet. This configuration was characteristic of all values of  $H/D$  less than 1.0.

It was deduced from the shapes of the 30°C and 40°C isothermals shown in Fig. 22 that when  $H/D$  was 0.25 there was a considerable upward deflection of the jet by the ground board.

The various temperature phenomena were substantiated by flow visualisation which will be discussed in the next section.

### 5.3 Flow visualisation

#### 5.3.1 Schlieren photographs and shadowgraph traces

A series of Schlieren photographs of the flow, covering the complete test range, and two shadowgraph traces for free air and for a value of  $H/D$  of 0.375, are shown in Figs. 26, 27, 28.

The changes in shape of the jet boundaries as the ground board height was decreased are clearly shown in the Schlieren photographs, which also show that near the ground the jet velocities were considerably decreased.

The photographs of the jet in free air and for  $\frac{H}{D} = 1.75$  show two regions of high horizontal density gradient, of similar shape to the grouped isothermals shown in Figs. 16, 17, 18. This effect was still apparent at  $\frac{H}{D} = 1$  but was less marked. The free air shadowgraph trace in Fig. 26 also shows the characteristic shape.

### 5.3.2 Temperature indicating paints

The only paints for which colour changes could be obtained were those having transition temperatures of 80°C and 115°C, even when the jet efflux temperature was raised to 180°C. The reason for this is unknown but it was not thought to be due to any fault in the paints.

The colour change boundaries obtained with the 80°C and 115°C indicating paints on splitter plates, showed similar shapes to the isothermals obtained from the thermocouple traverses, but did not supply any additional information. The colour change boundaries obtained with the 80° indicating paint on the ground board were circular, thus indicating symmetrical temperature distribution.

### 5.3.3 Wool tuft probe

The flow patterns obtained by the wool tuft probe are shown in Figs. 29 and 30, for the jet in free air, and for values of  $H/D$  of 1.5 and 0.5. These diagrams show three distinct phases of the flow.

For values of ground proximity parameter greater than 2 a region of circulation extended for 1.0 in. below the centre-body. The flow then became uniform before being influenced by the ground board. The free air case is shown in Fig. 29.

H

When the ground board was at  $\frac{H}{D} = 1.5$  there was a larger region of circulation under the centre-body, extending a distance of 1.5 in. A region of general turbulence separated this and the extensive circulation above the ground board.

The circulation extended from the centre-body to the ground board for values of ground proximity parameter less than 1.0. This is

H

illustrated for  $\frac{H}{D} = 0.5$ .

D

The variation of temperature under the centre-body with ground proximity can be accounted for by reference to these flow patterns. When the jet was in free air or at large values of  $H/D$ , circulation was confined to a small region under the centre-body. Hence the circulating air was at a high temperature as it came directly from the unmixed hot jet. At intermediate values of the ground proximity parameter (i.e., 1.5 and 1.0), the circulation was more extensive and air reached the underneath of the nozzle from the lower, cooler regions of the jet, thus causing the temperature to fall. Although, at smaller values of  $H/D$ , the circulation extended from the nozzle to the ground board, the close proximity of the latter served to contain the heat in the central region, causing the centre-body temperature to rise again.

### 5.3.4 Oil film

Oil film splitter plate techniques served to verify the wool tuft flow patterns. In particular the splitter plates showed the flow to be uniform for 'h' greater than 2.0 in. in the free air case, and also the extent of circulation under the nozzle. Three-dimensional effects masked the flow patterns to some extent, consequently they are not included in this report.

## 5.4 Jet velocity and total heat (for the jet in free air)

The temperature traverses and the total and static pressure traverses were used to calculate the velocity profiles at various stations in the jet. From the velocity profiles shown in Fig. 23, it can be seen that

the/

the peak velocity moved inwards from under the jets to the centreline of the nozzle as 'h' increased. Visualisation of the flow showed that total and static pressure traverses could not be made closer than 2.0 in. to the nozzle with the apparatus used.

In an attempt to establish the accuracy of the temperature and pressure measurements in the jet, the total heat passing per second above ambient temperature, was calculated at the nozzle exit and at 8.0 in. from the exit. At the two positions it was found to be respectively, 4.3 B.t.u./sec and 3.9 B.t.u./sec. Heat losses in a jet of this nature expanding into free air are negligible, and these reasonably close values of total heat indicate that errors in measurement were small.

## 6. Conclusions

6.1 The jet configuration used gave a large augmentation of thrust when in close proximity to the ground.

6.2 The thrust augmentation effect was the same when both jets were cold, and when the inner jet was heated.

6.3 When the jet was ejecting into free air there was a considerable pressure drag on the base areas of the nozzle. For a practical engine this latter effect would be of more significance than the thrust augmentation effect. The reason for this is that the engine would not, in a normal aircraft configuration, come close enough to the ground for the thrust augmentation to be appreciable. On the other hand the pressure drag would reduce the overall efficiency of the engine. It is possible that streamlining the nozzle bases or angling the jets inwards would help to reduce this drag.

6.4 The thrust augmentation was accompanied by radical changes of the temperature distribution in the jet. In particular, the temperature on the base of the nozzle centre-body changed considerably with ground proximity.

6.5 The air heater proved very satisfactory for the conditions used during the tests, but for higher mass flows a different heating method would be required. A possible design would be a heat exchanger, using as a heating fluid, the hot products of combustion from an injection burner of the type used in the present heater.

## Acknowledgements

The authors wish to express their thanks to the members of the academic and workshop staff of the Department of Aeronautical Engineering. Particular thanks are extended to Mr. T. V. Lawson and Mr. T. Cook for their continued help and encouragement throughout the investigation.

The authors also wish to express their thanks to Mr. Eccleshare of the South Western Gas Board, for his help in connection with the air heater.

---

References

<u>No.</u>	<u>Author(s)</u>	<u>Title, etc.</u>
1	U. H. von Glahn	Exploratory study of ground proximity effects on thrust of annular and circular nozzles. N.A.C.A. Tech. Note 3982, April, 1957.
2	B. W. J. Childes and I. A. Fisher	The effects of ground proximity on the thrust from an annular nozzle. University of Bristol, Department of Aeronautical Engineering, Report No.42, 1959.
3	H. B. Squire and J. Troncner	Round jets in a general stream. A.R.C. R. & M. 1974, January, 1944.
4	S. Pai	Fluid Dynamics of Jets. D. Van Nostrand Company, Inc., 1954.
5	R. R. Burley and L. Bryant	Experimental investigation of coaxial jet mixing of two subsonic streams, at various Mach number and diameter ratios, for three configurations. N.A.S.A. Memo. 12-21-58E, February, 1959. TIL 6229.
6	J. H. Preston	The three-quarter radius pitot tube flow meter. The Engineer, Vol.190, p.400, 1950.
7	W. E. Francis and B. Jackson	Jet burner design for pressure efficiency. The Gas Council, Research Communication, G.C.44, 1957.

References to Manufacturers

8	Marco S.B.28.D. Resin - Scott Bader & Co. Ltd., 109, Kingsway, London, W.C.2.
9	Thermindex Temperature Indicating Paints - J. M. Steel & Co. Ltd., Kern House, 36/38, Kingsway, London, W.C.2.

APPENDIX

Design and Development of the Air Heater

---

Four methods of heating the required volume of air were reviewed. These were:- electrical heating, liquid fuel combustion, gas heating, and the heat exchanger method, with an external heat source. Of these the gas heater method was chosen as being probably the easiest approach to the problem. Electric heating was discarded because of the large capacity needed and difficulty of control. It was considered that the heat exchanger method would require too much development work and would also be difficult to control, while a liquid fuel combustion chamber would have given too high a temperature.

The basic problem of gas heating was to induce the gas into the combustion chamber against the high back pressure of the main air supply. Pressurisation of the normal town gas supply was impracticable, as also was the use of "bottled gas". The latter could be delivered at a slightly higher pressure than the normal gas supply, but the difference was negligible in relation to the back pressure involved.

In the initial design, the gas entered the heater through a nozzle in the inner 2.0 in. diameter flame tube, which can be seen in Fig. 7. It was hoped that the high velocity past the exit of this tube would reduce pressure in the combustion area sufficiently to allow the gas to enter. While this system worked satisfactorily with the back pressure removed, the constriction at the end of the heater tube created sufficient back pressure to prevent entry of the gas.

To overcome this difficulty a gas injection system was developed, whereby a high velocity secondary airstream was used to induce the gas into the heater. Injectors of this type have been studied before<sup>7</sup>, but to the authors' knowledge, have not been utilised with such high air injection pressures, and for systems with high back pressures.

Fig. 7 shows the final design of the heater. During the initial test the following faults were apparent: firstly, oscillatory combustion occurred at the working pressure, and secondly, the air temperature could not be reduced to the design temperature of the fibreglass nozzle (200°C).

As a first attempt to remedy these faults the injection air pressure was raised from 80 lb/in.<sup>2</sup> to 130 lb/in.<sup>2</sup>; although this allowed higher mass flows to be obtained it did not cure the combustion resonance. Shortening the combustion chamber and removing the inner flame tube, were also tried to no effect. By reducing the air injector nozzle diameter from  $\frac{1}{8}$  in. to  $\frac{3}{32}$  in. it was found possible to obtain steady combustion at a pressure slightly below the required working pressure of 5 lb/in.<sup>2</sup>, but the temperature was still too high.

It was next decided that the complete combustion chamber-mixing tube assembly would have to be scaled down, retaining the  $\frac{3}{32}$  in. diameter air injector nozzle. The original dimensions were:-



- 16 -

The temperature was now variable between 100°C and 200°C at the working pressure of 5 lb/in.<sup>2</sup>, without oscillatory combustion occurring. At a pressure 50% greater than the working pressure, unstable combustion still occurred, above this pressure the flame was extinguished.

Throughout the tests the heater and the ignition system functioned satisfactorily, the total running time being in the order of 40 hours.

---

ES

FIG.1.

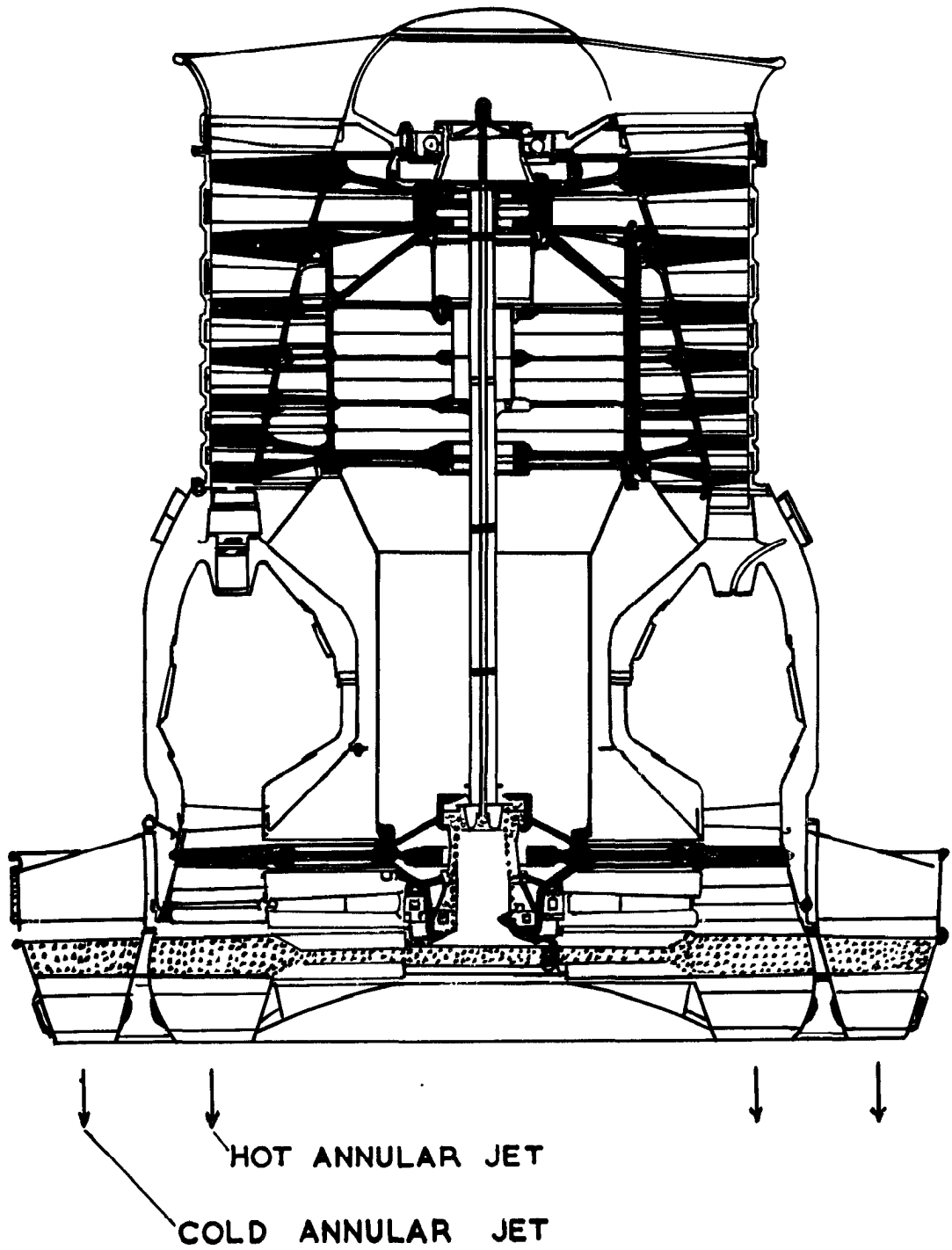
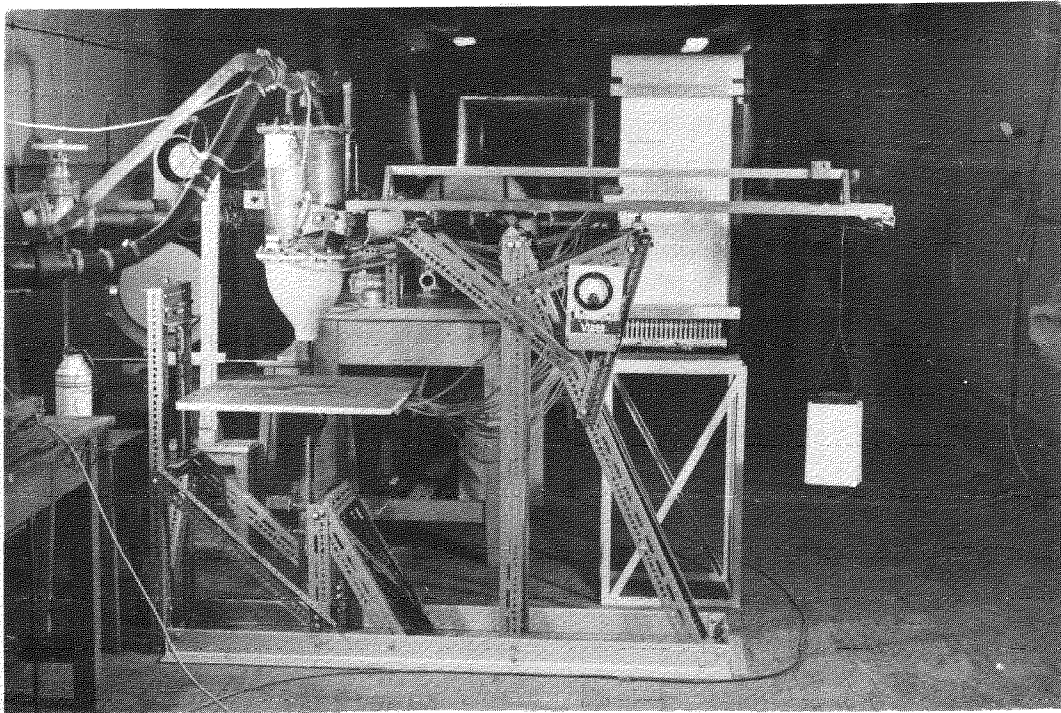


FIG.1. DESIGN FOR A SPECIALISED  
LIFTING ENGINE PROPOSED BY  
BRISTOL SIDDELEY ENGINES LTD

FIGS. 2 & 3

FIG. 2



**GENERAL VIEW OF THRUST BALANCE,  
NOZZLE ASSEMBLY, AND GROUND BOARD.**

FIG. 3

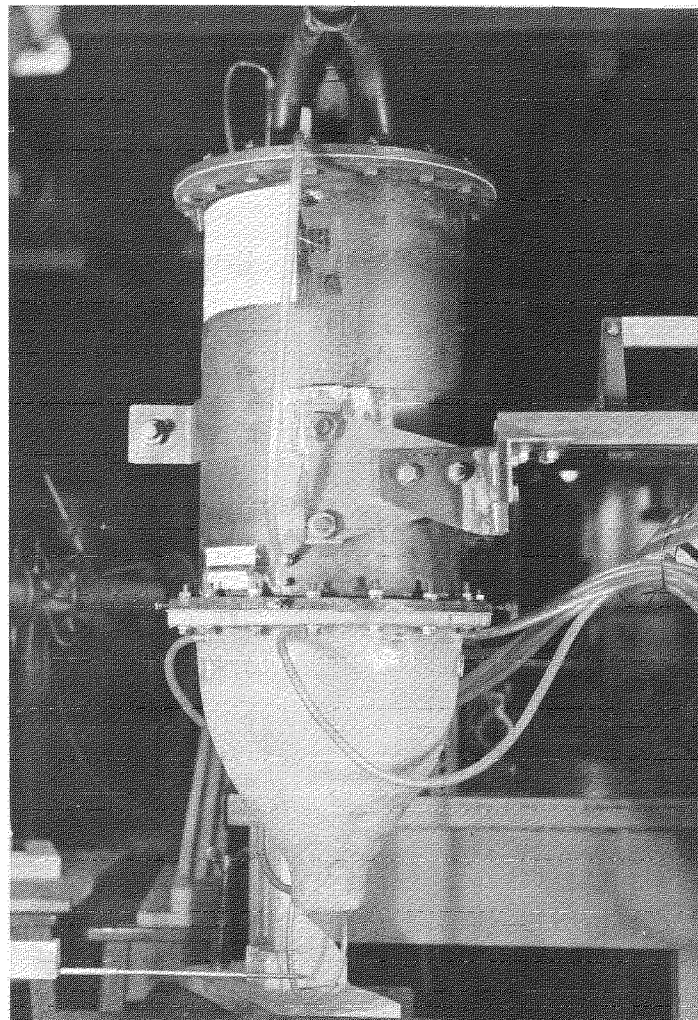
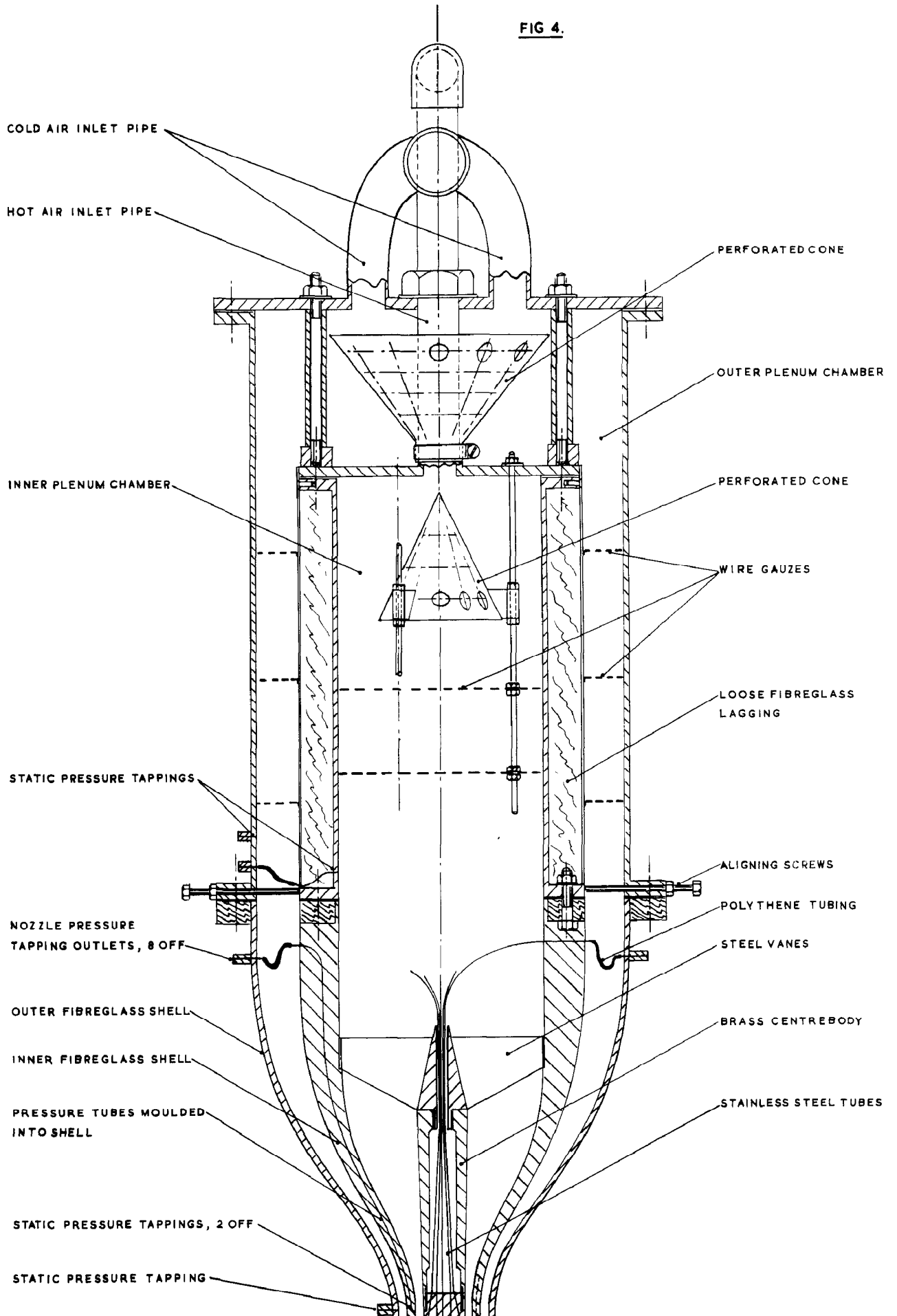
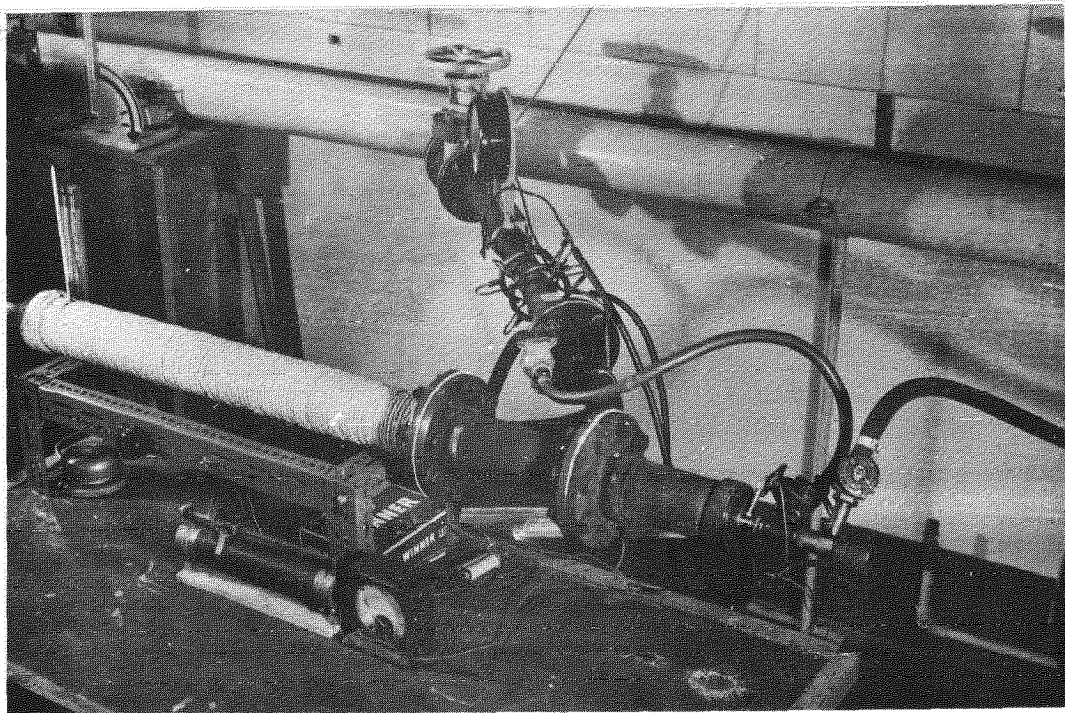


FIG 4.



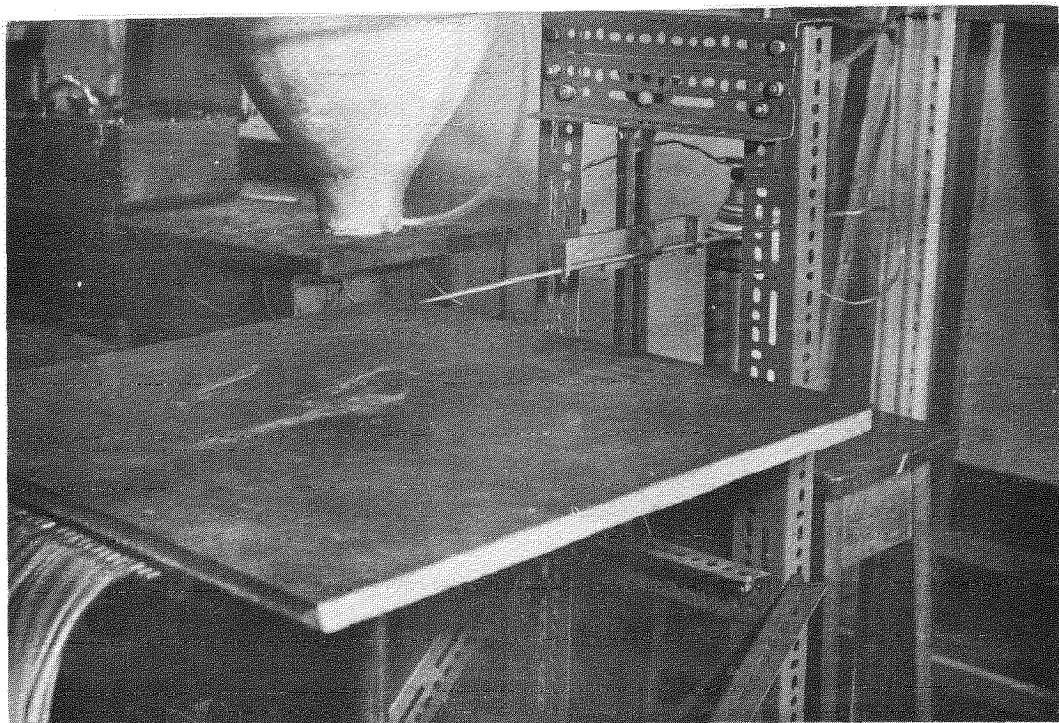
FIGS. 5 & 6

FIG. 5



AIR HEATER ARRANGEMENT.

FIG. 6



GROUND BOARD, TRAVERSING RIG,  
AND THERMOCOUPLE PROBE.

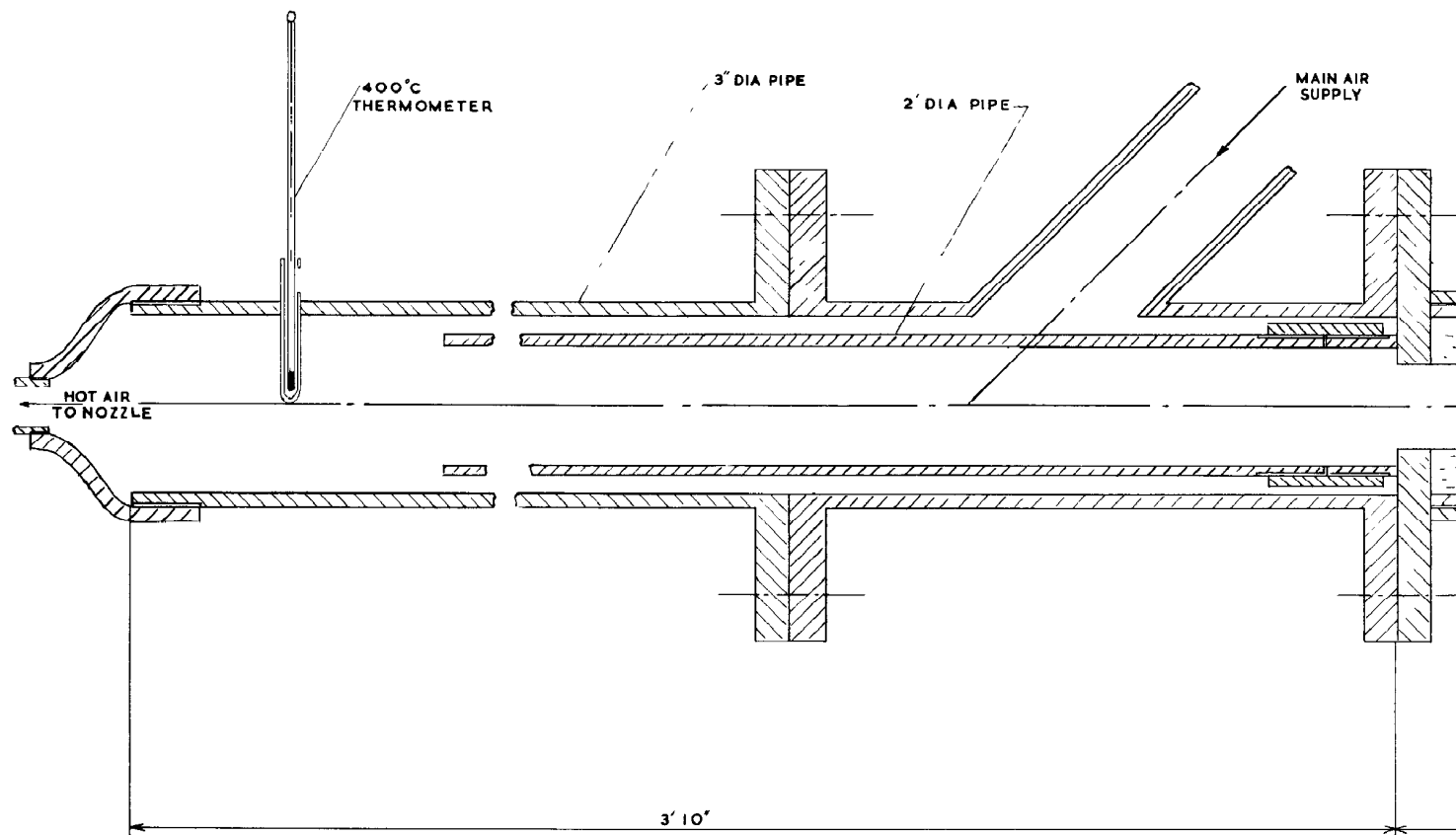


**FIG. 7. AIR HEATER**

**FIGS. 8. & 9.**

**FIGS. 8. 9**

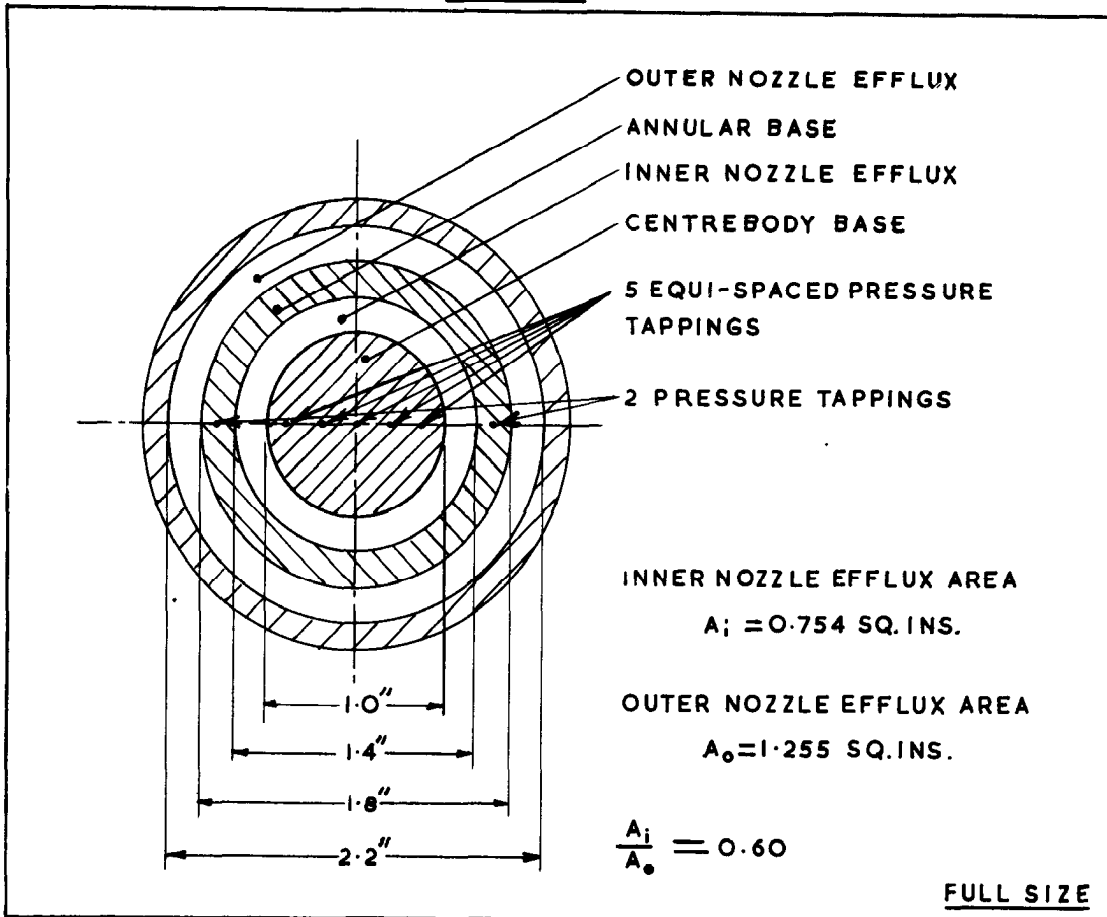


**FIG. 8. NOZZLE DIMENSIONS**

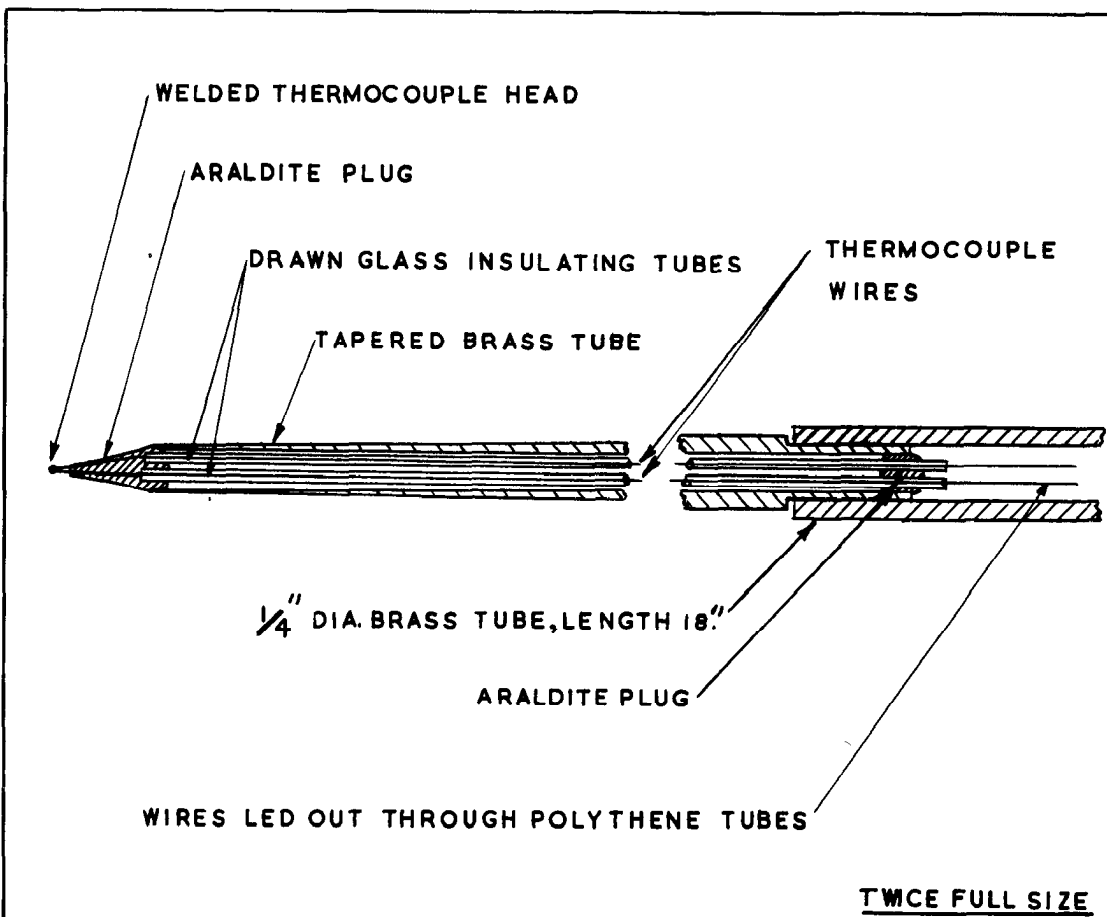


**FIG. 9. THERMOCOUPLE PROBE**

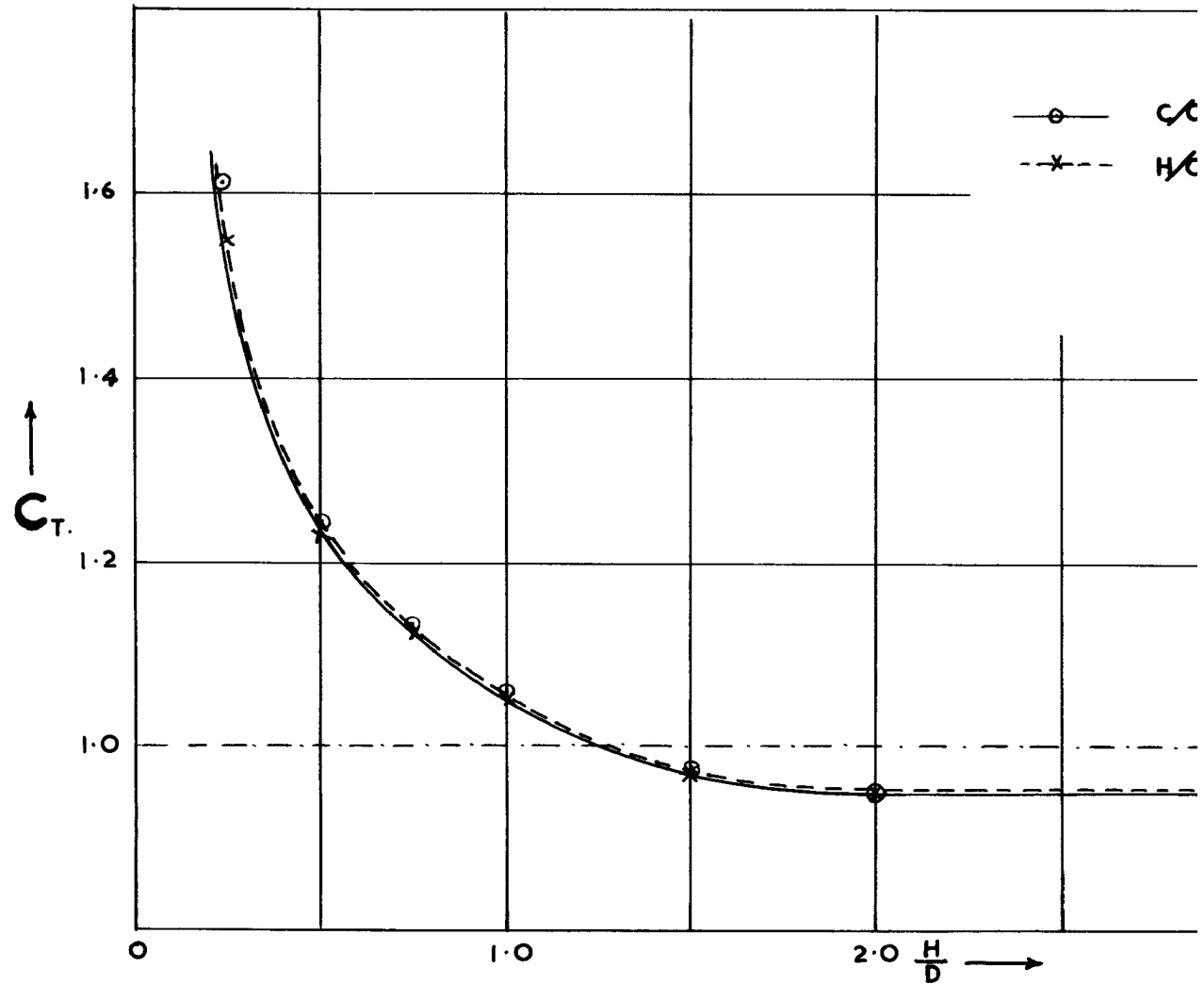
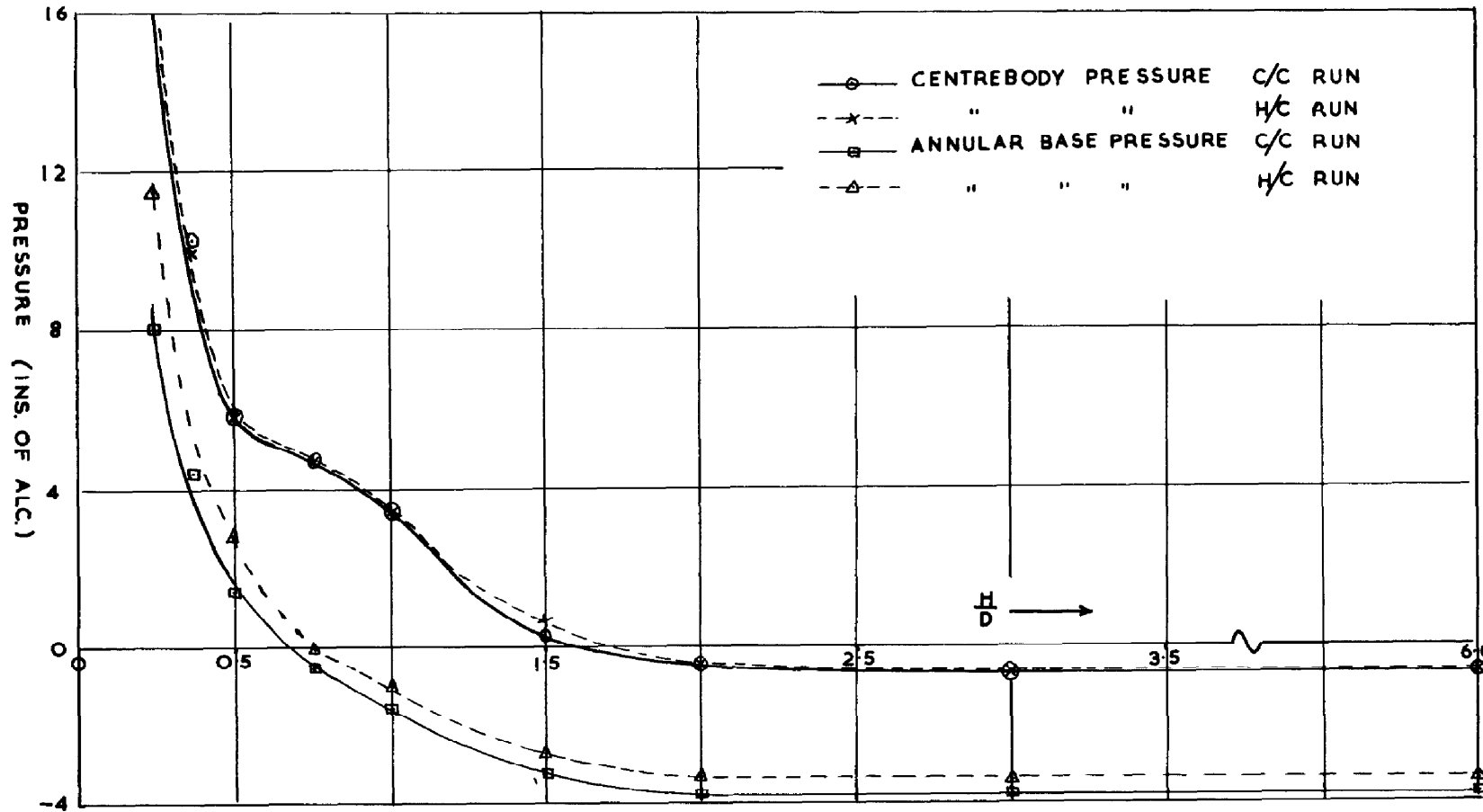


FIG. 10. VARIATION OF THRUST COEFFICIENT  
HEIGHT PARAMETER  $\frac{H}{D}$





**FIG. II.**

**FIG. II. VARIATION OF PRESSURE UNDER CENTRBODY AND ANNULAR BASE WITH HEIGHT PARAMETER  $\frac{H}{D}$**

**FIG. II.**

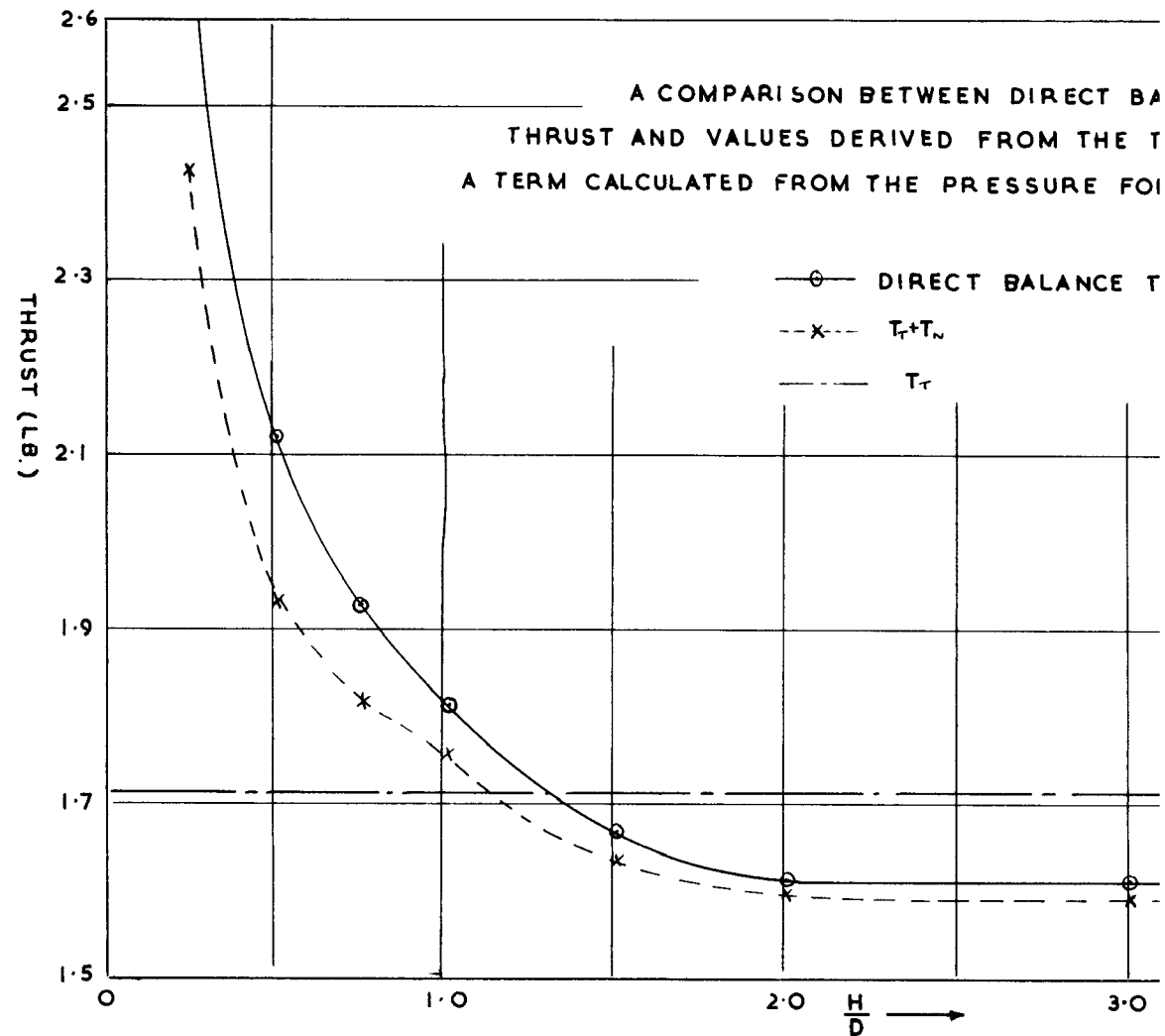


**FIG.12. VARIATION OF THRUST WITH HEIGH**  
**H/C RUN**

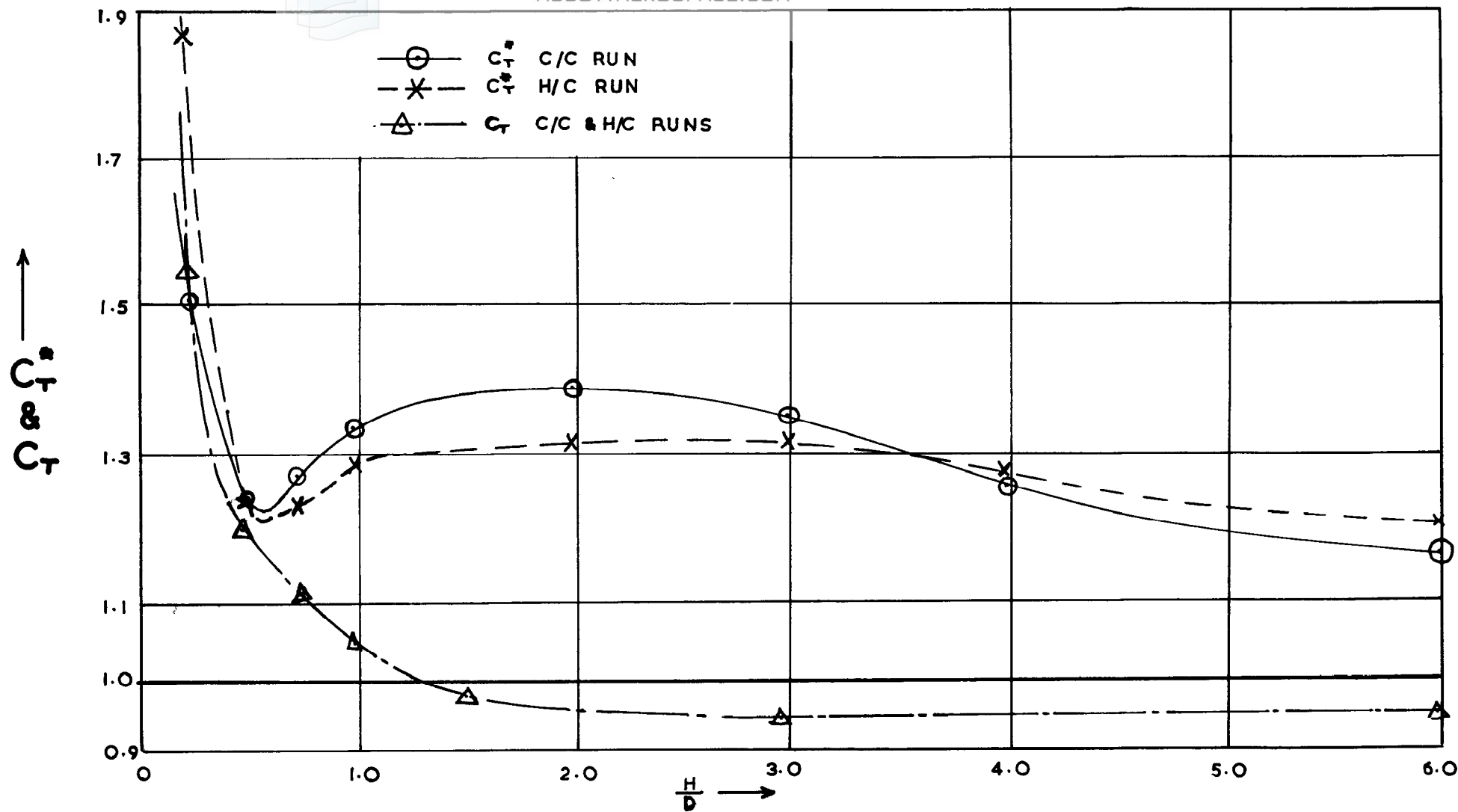


FIG. 15. COMPARISON OF THE VARIATION OF THRUST  
COEFFICIENTS  $C_T^*$  &  $C_T$  WITH HEIGHT PARAMETER  $H/D$

FIG. 15.

FIG. 15.

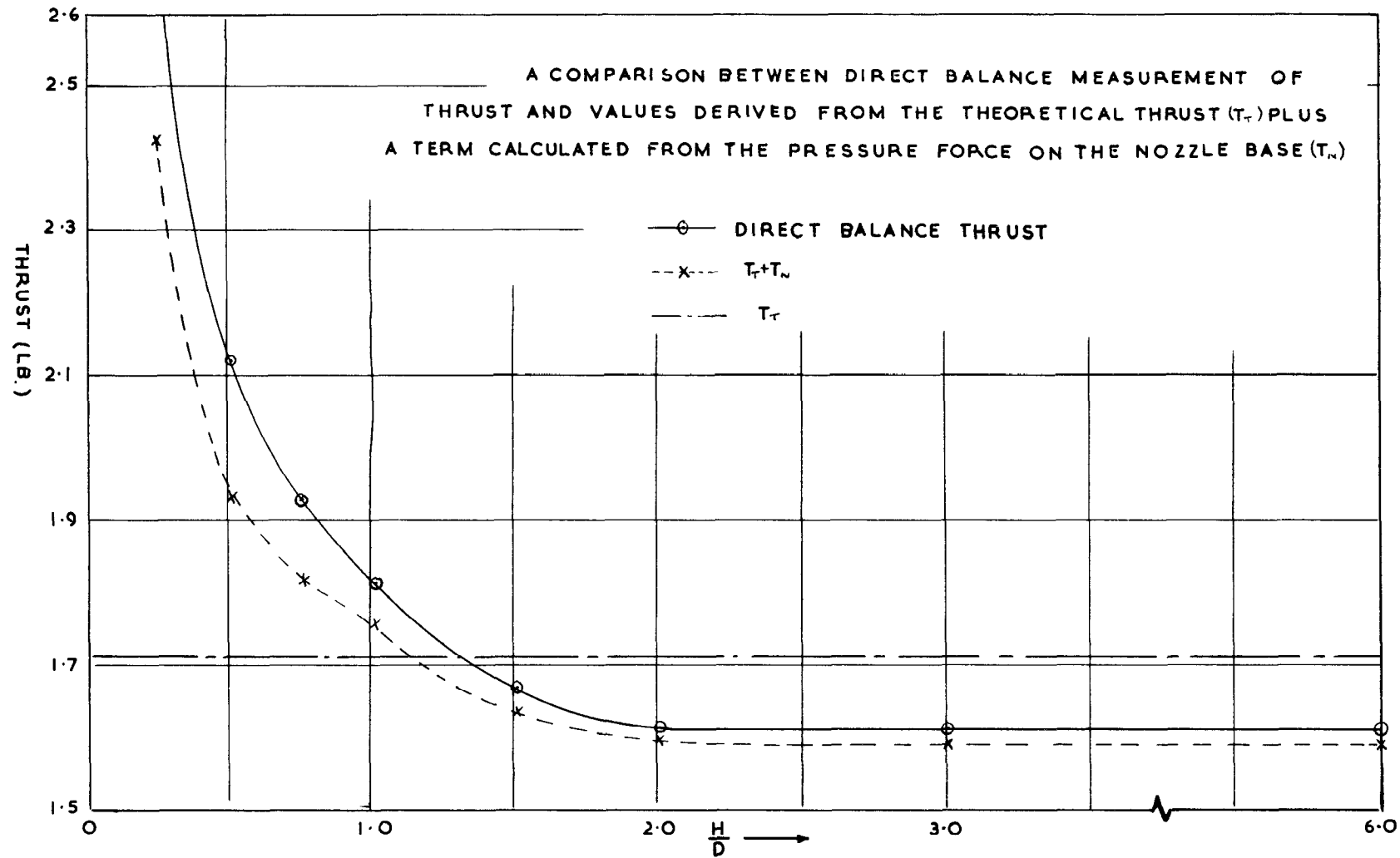


FIG.12.

FIG.12. VARIATION OF THRUST WITH HEIGHT PARAMETER  $\frac{H}{D}$   
H/C RUN

FIG.12.

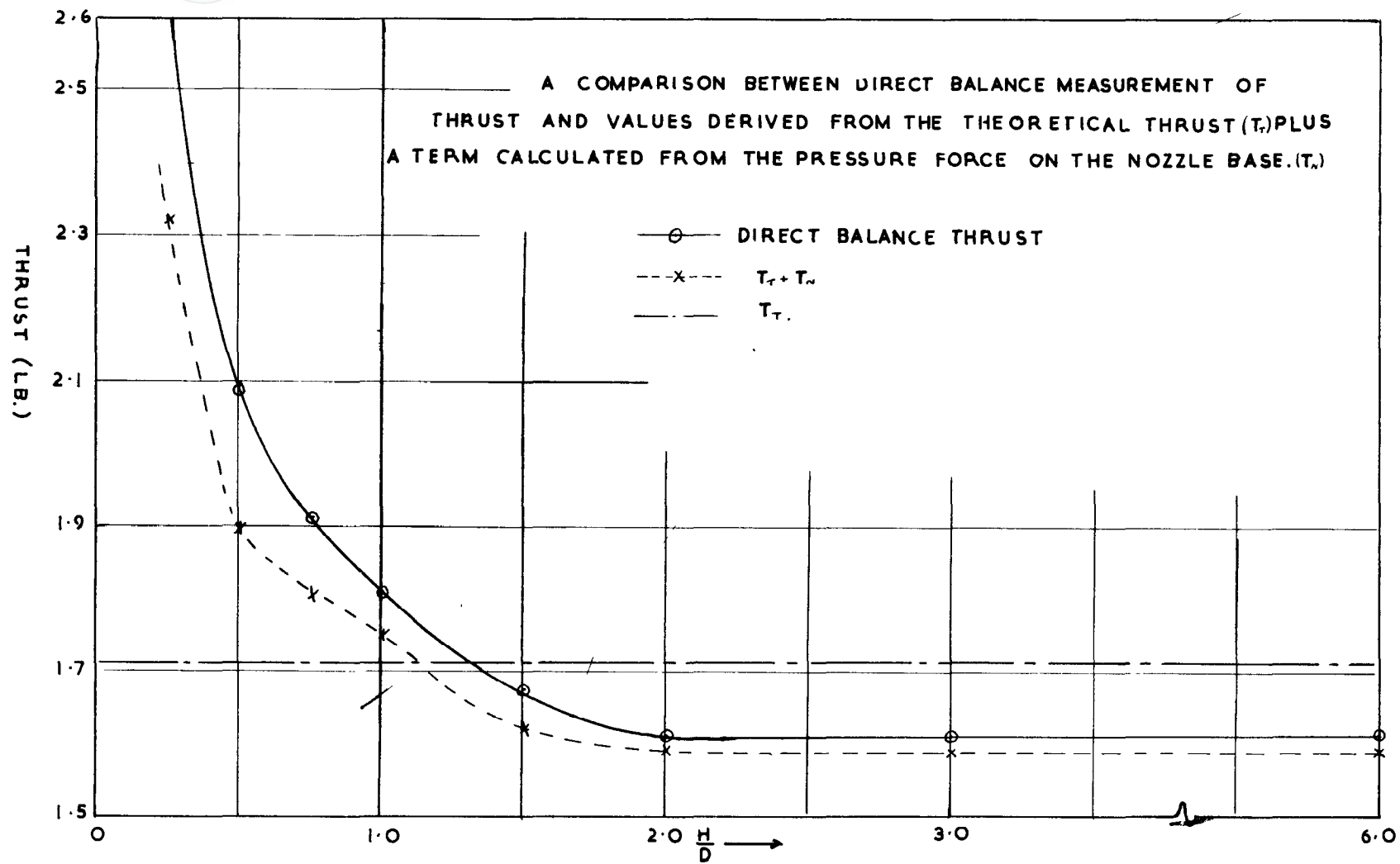


FIG. 13.

FIG. 13: VARIATION OF THRUST WITH HEIGHT PARAMETER  $\frac{H}{D}$   
C/C. RUN

FIG. 13.

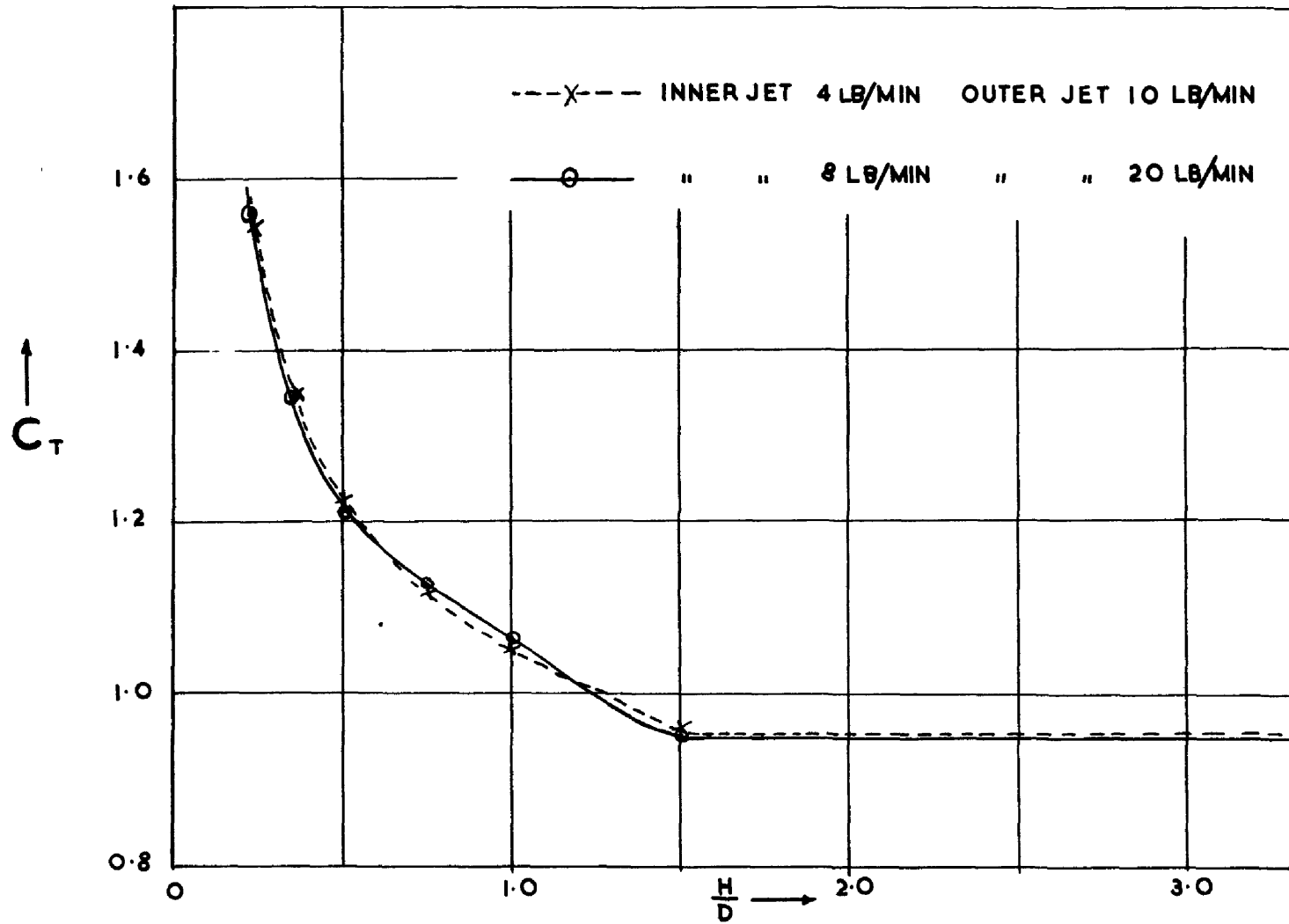
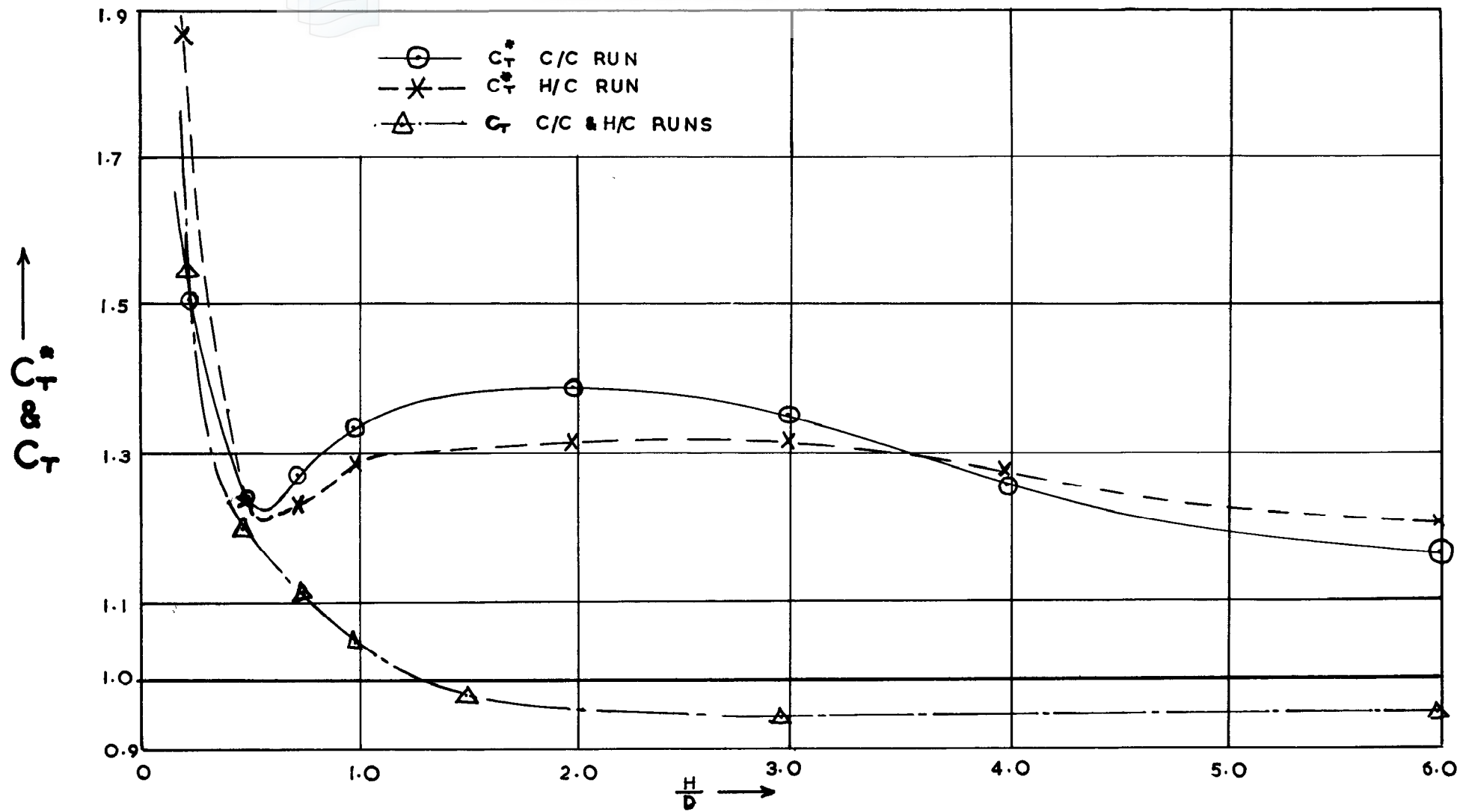


FIG. 14. VARIATION OF THRUST COEFFICIENT (  
PARAMETER  $\frac{H}{D}$  C/C. RUN



**FIG. 15. COMPARISON OF THE VARIATION OF THRUST  
COEFFICIENTS  $C_T^*$  &  $C_T$  WITH HEIGHT PARAMETER  $H/D$**

FIG. 15.

FIG. 15.

FIG. 16.

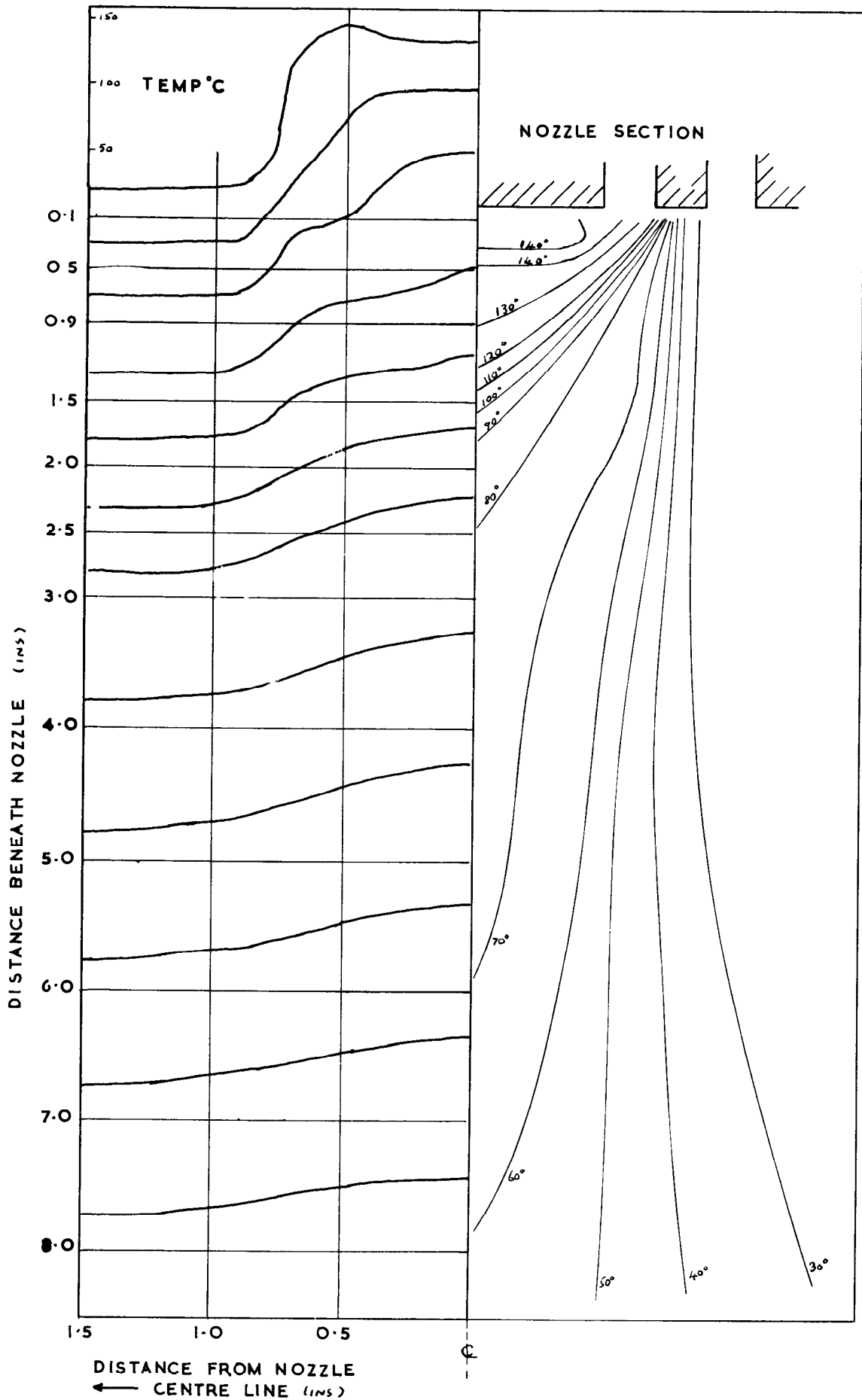


**FIG. 16. TEMPERATURE DISTRIBUTION  
 WITH GROUND BOARD AT  $\frac{H}{D} = \infty$**



**FIG.17.**

**FIG.17**

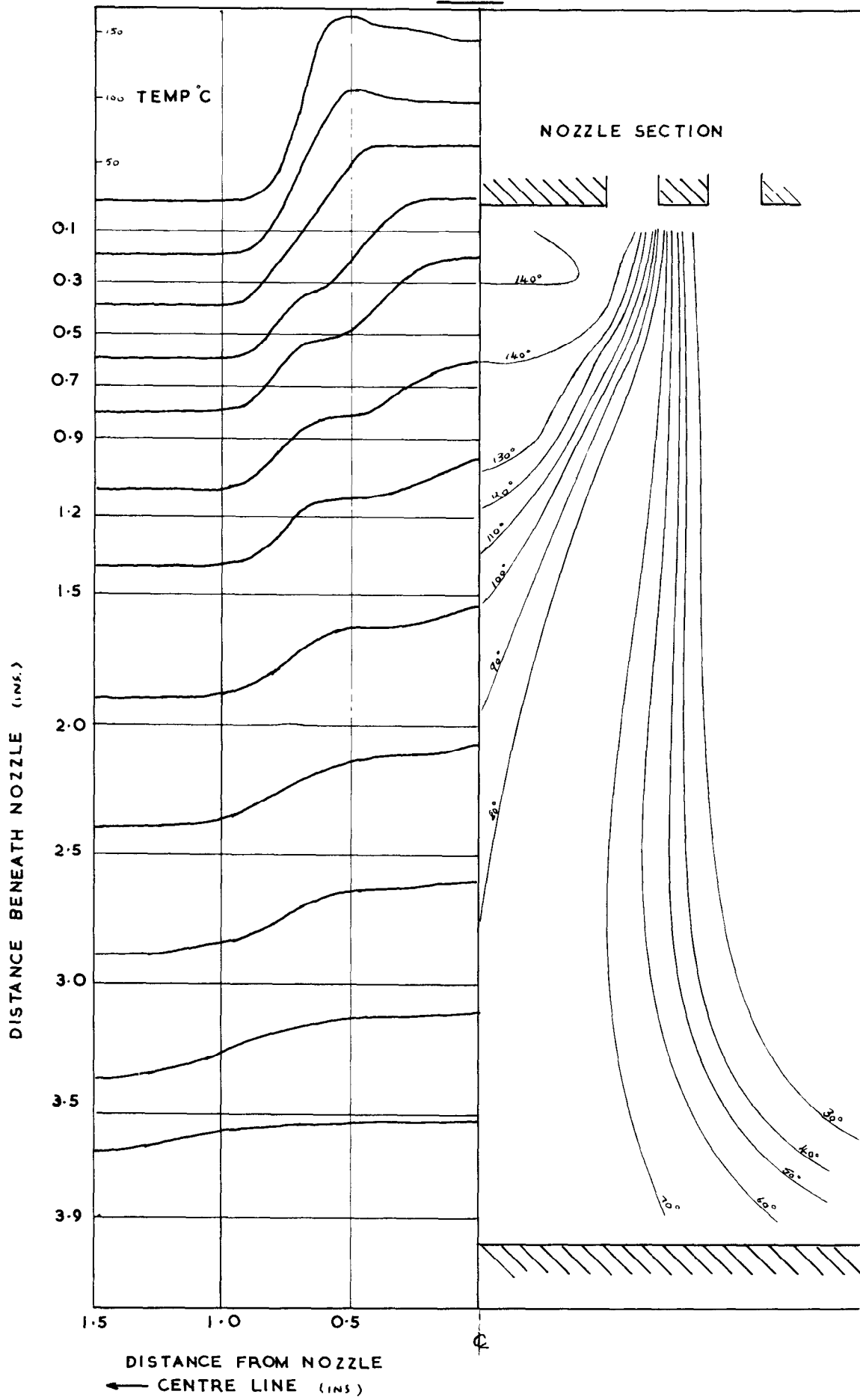


**FIG. 17. TEMPERATURE DISTRIBUTION WITH GROUND BOARD AT  $\frac{H}{D} = 2.0$**

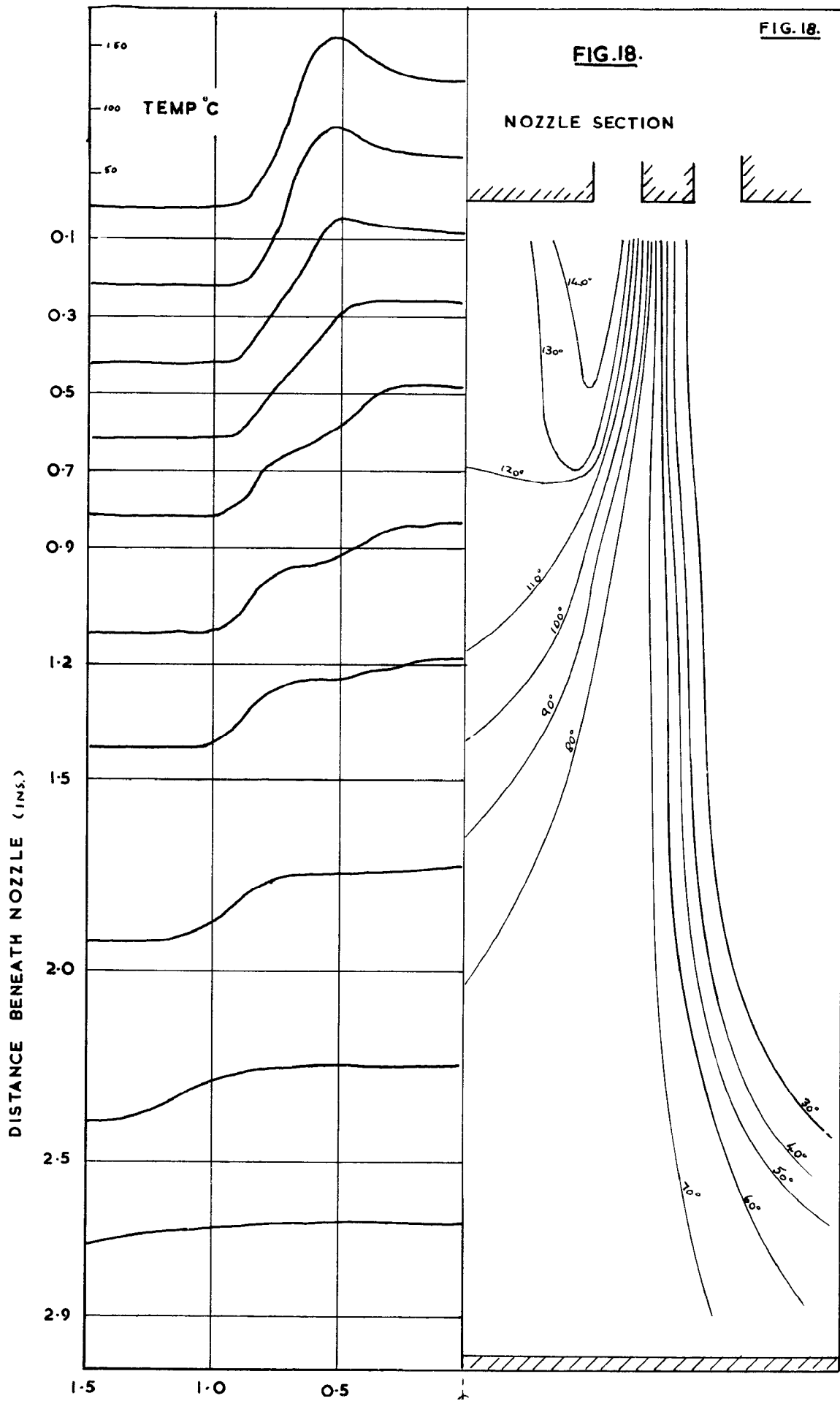
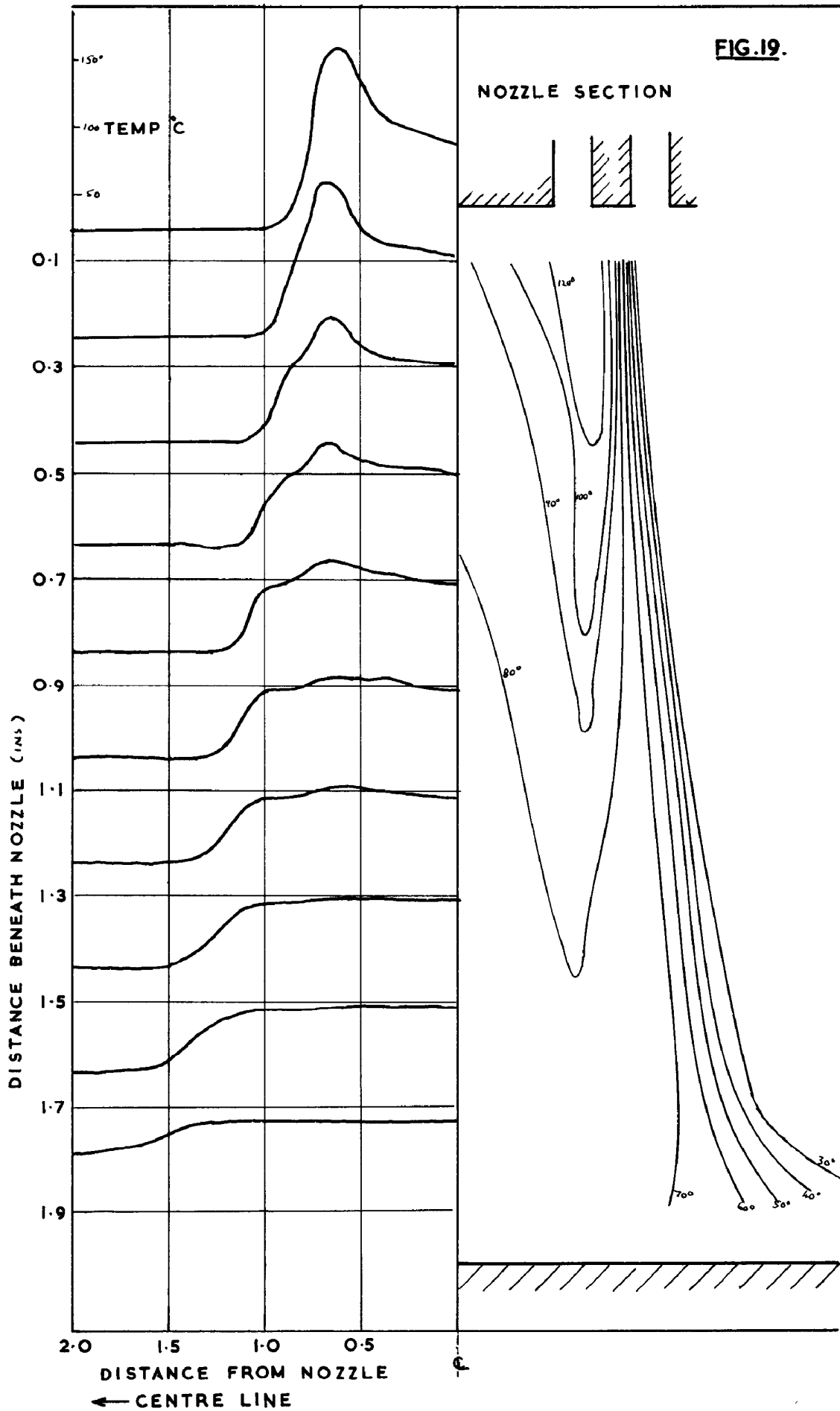


FIG.19.



**FIG.19. TEMPERATURE DISTRIBUTION**

**WITH GROUND BOARD AT  $\frac{H}{D} = 1.0$**

**FIG. 20.**

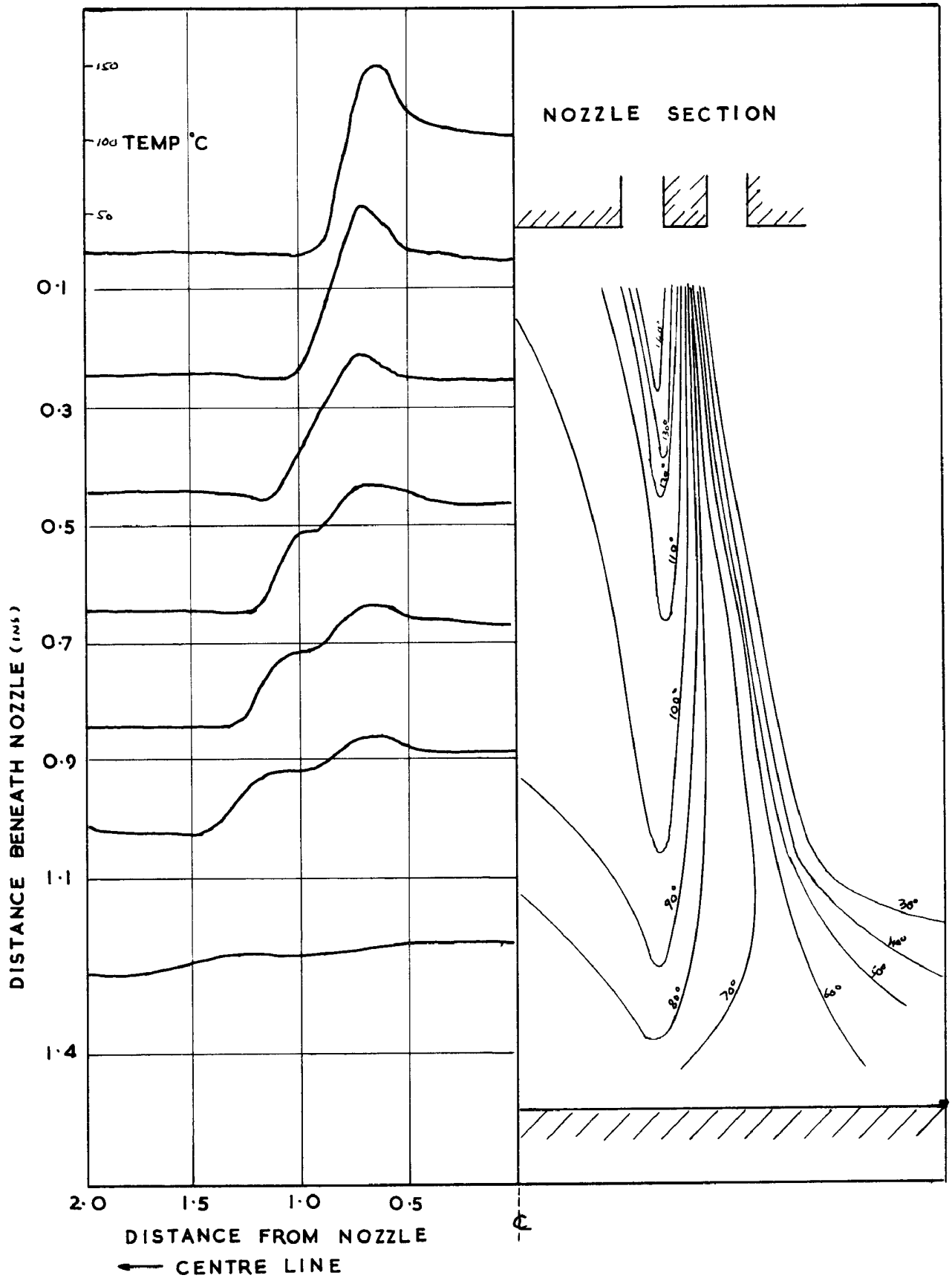


**FIG. 20. TEMPERATURE DISTRIBUTION  
 WITH GROUND BOARD AT  $\frac{H}{D} = 0.75$**

FIG. 21.

FIG. 21.

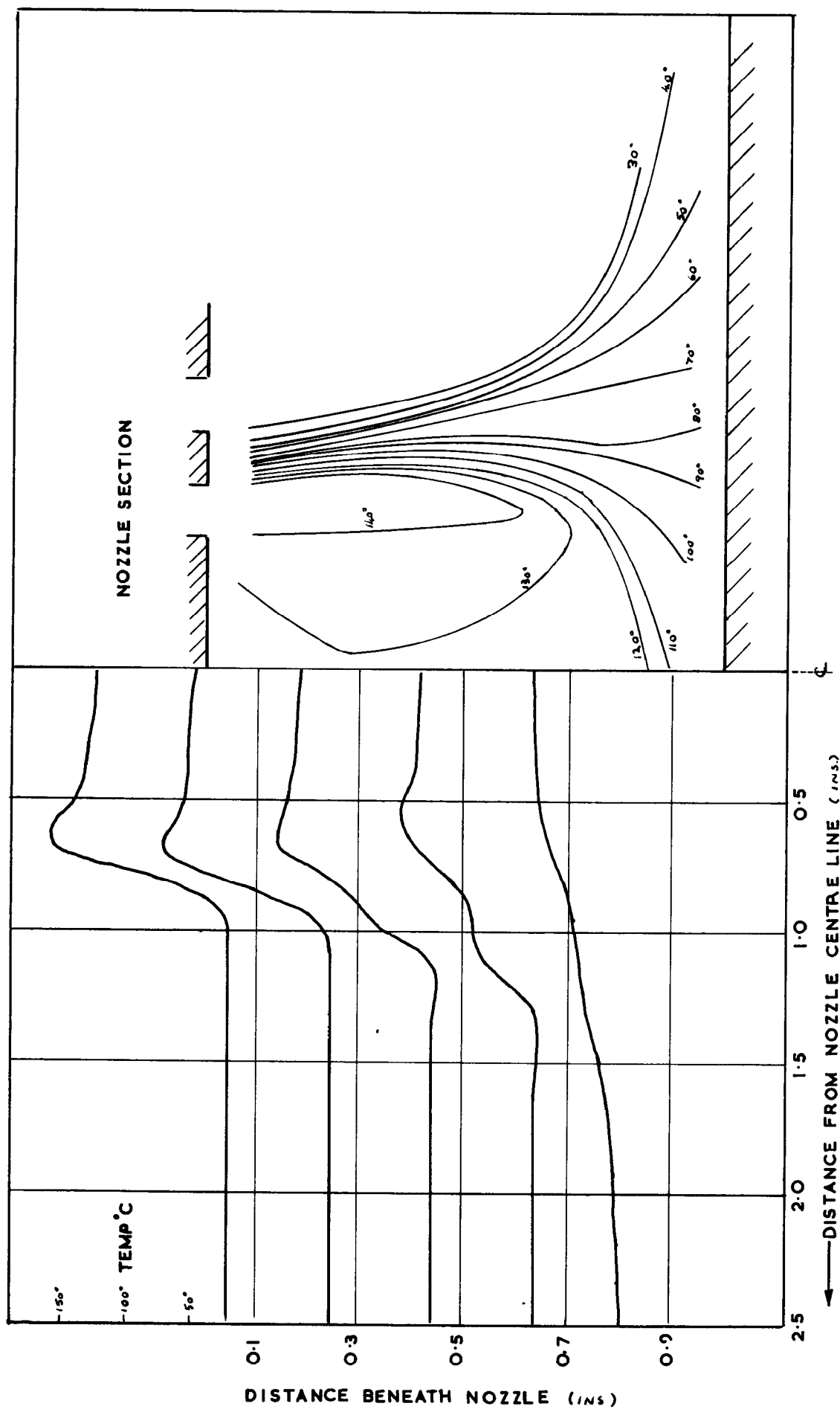
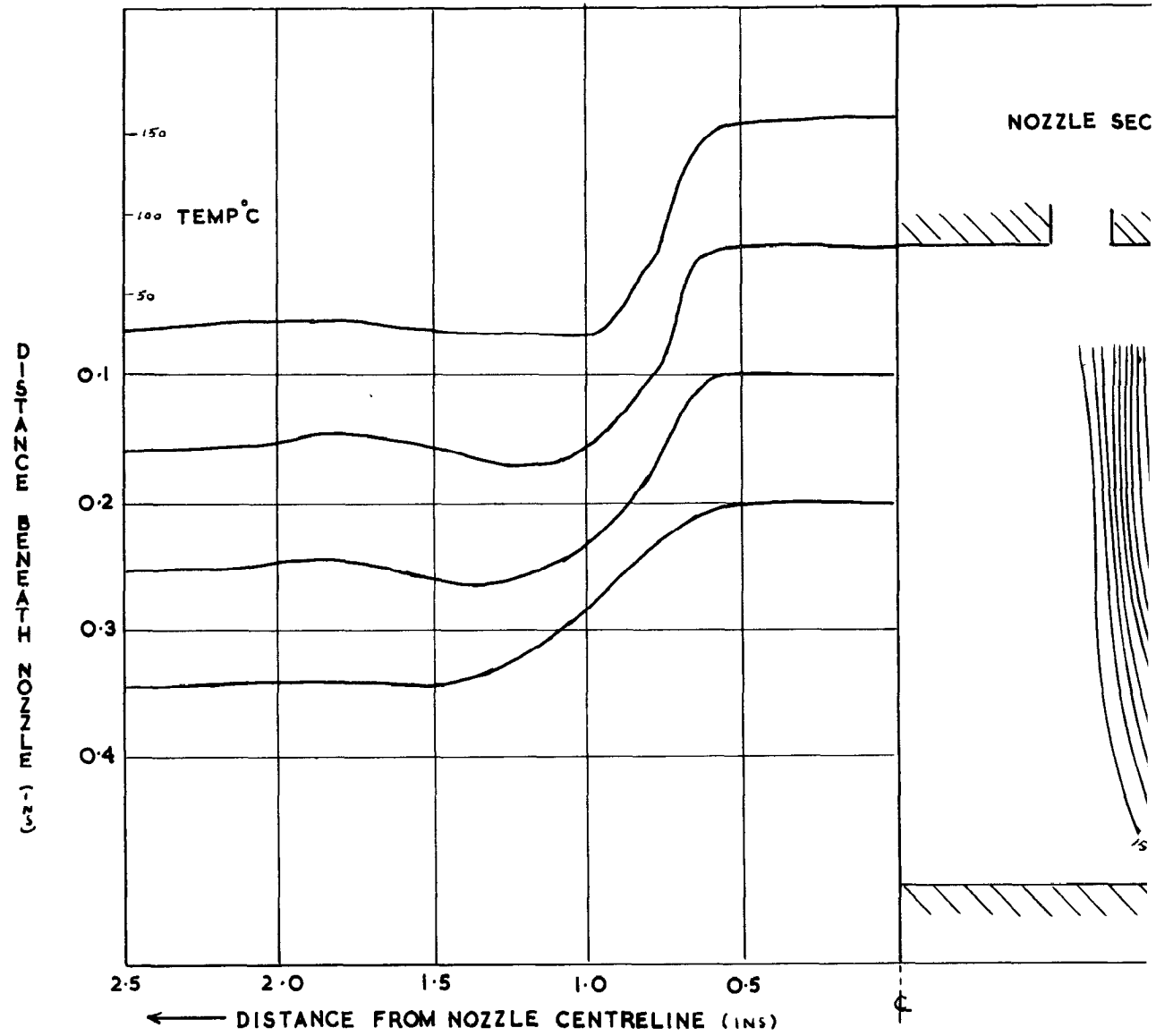


FIG. 21. TEMPERATURE DISTRIBUTION WITH GROUND BOARD AT  $H/D = 0.5$



**FIG. 22. TEMPERATURE DISTRIBUTION WITH GRO**

FIG. 23.

FIG. 23.

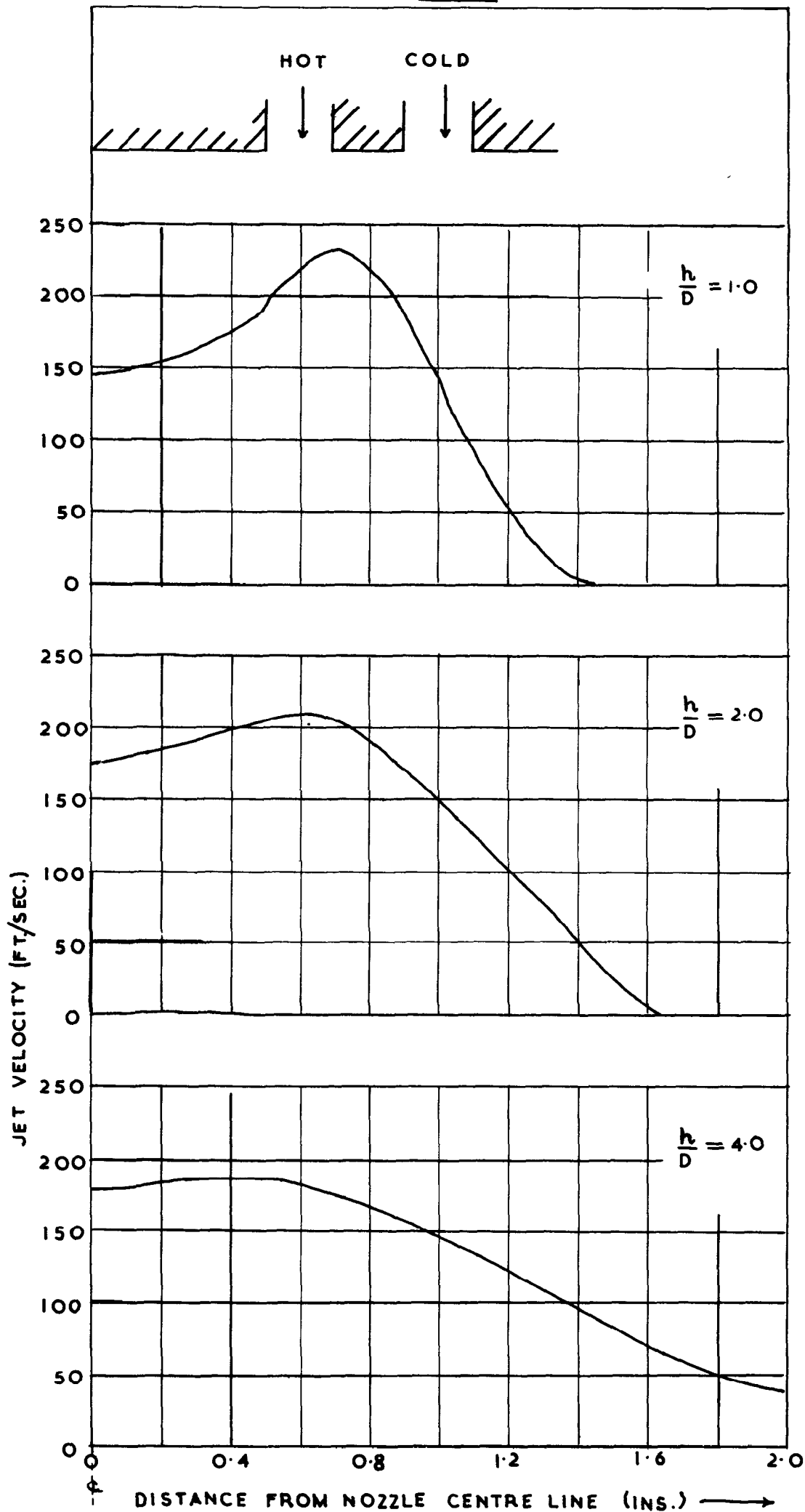


FIG. 23. VELOCITY PROFILES FOR THE  
 JET IN FREE AIR, HOT RUN

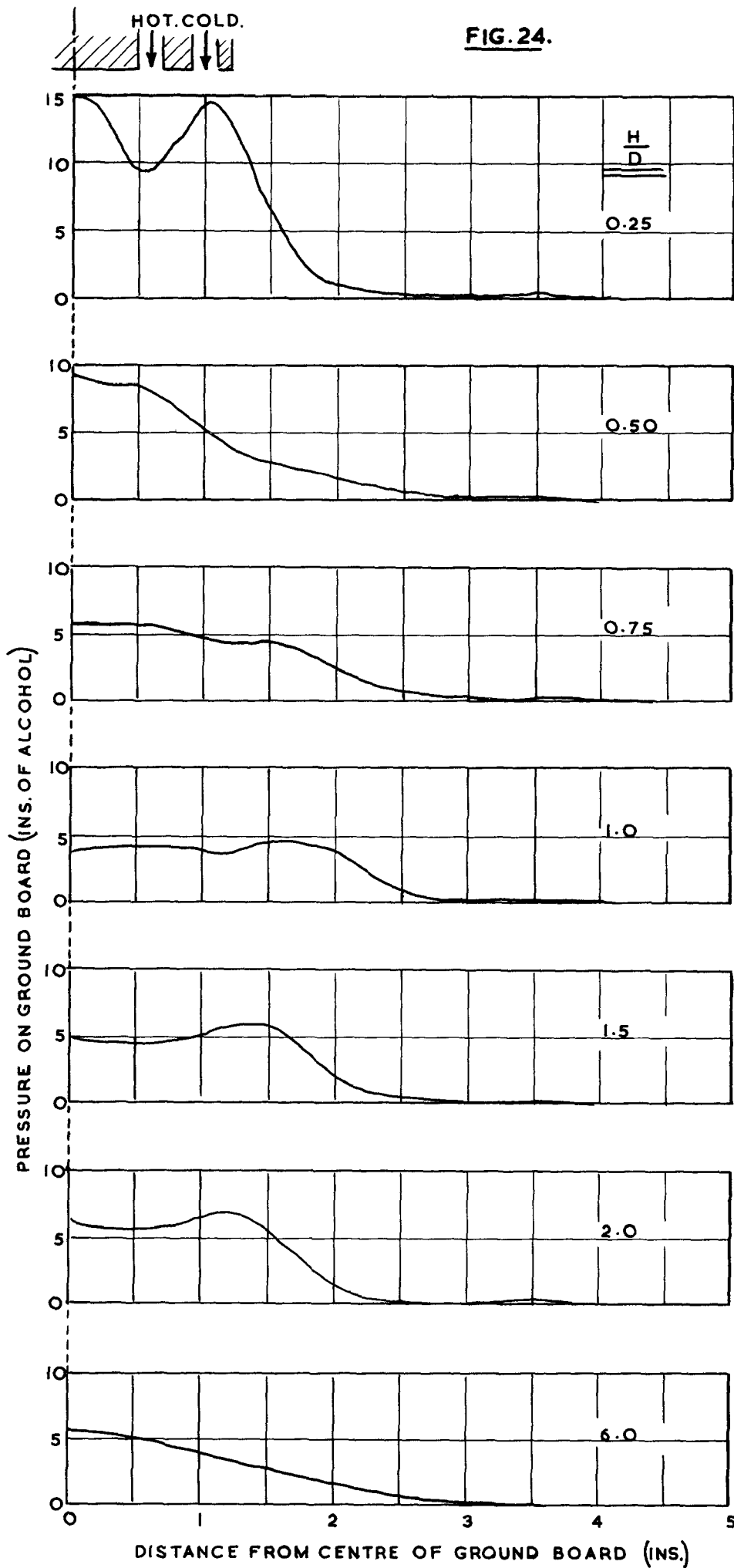
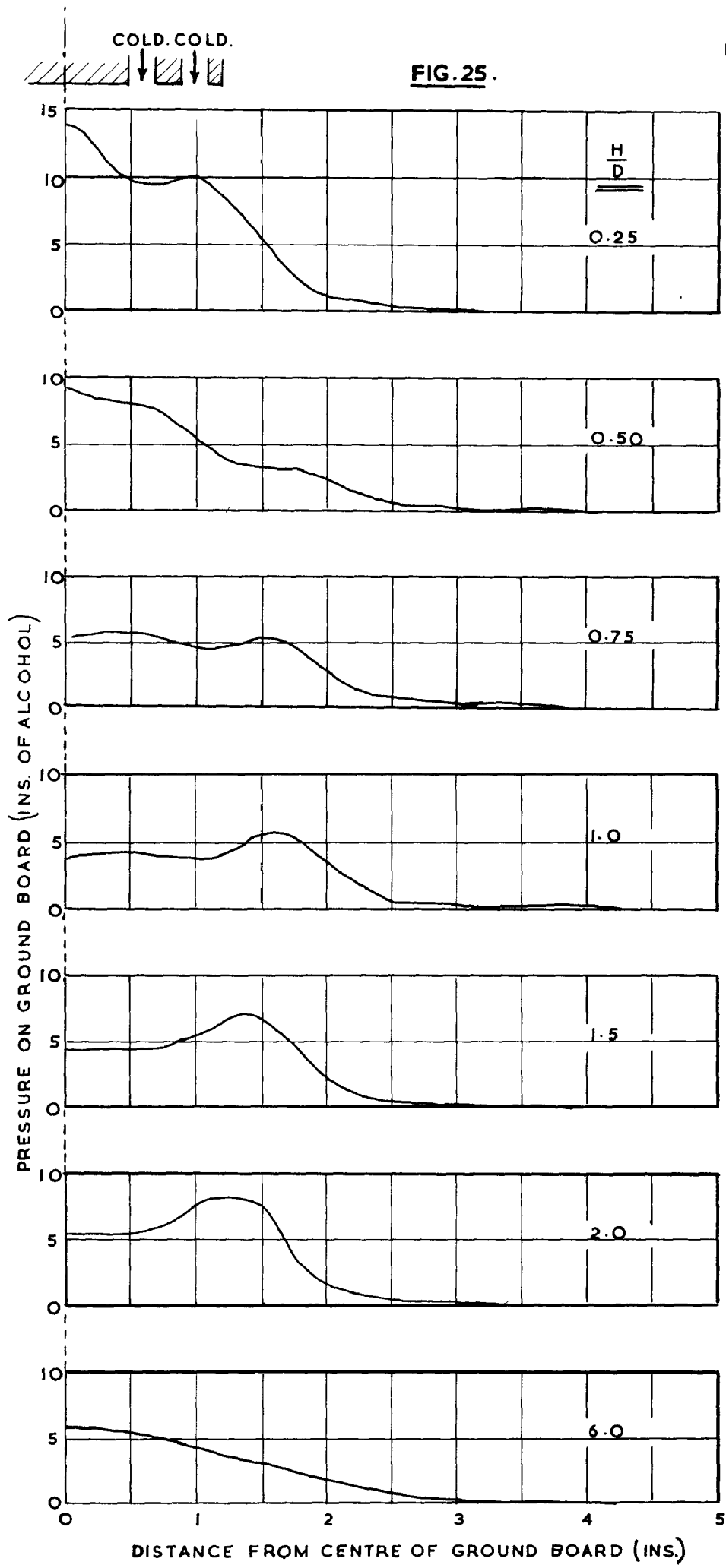


FIG. 24.

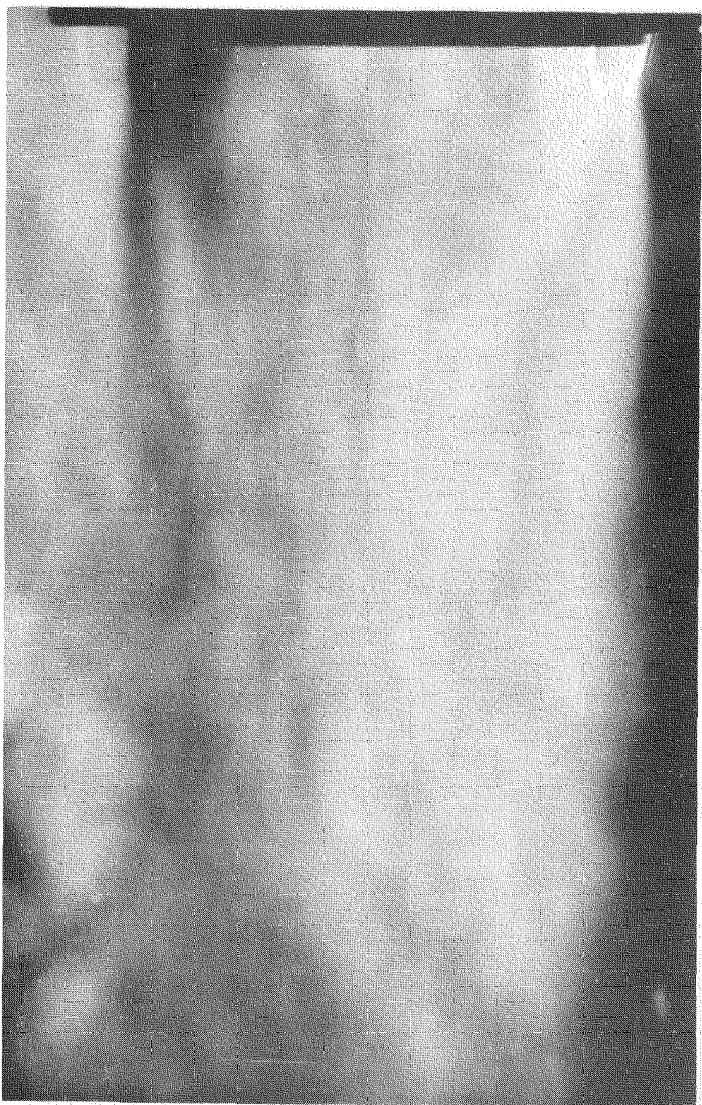
FIG. 24.

FIG. 24. PRESSURE DISTRIBUTION ON THE GROUND BOARD, H/C RUN.

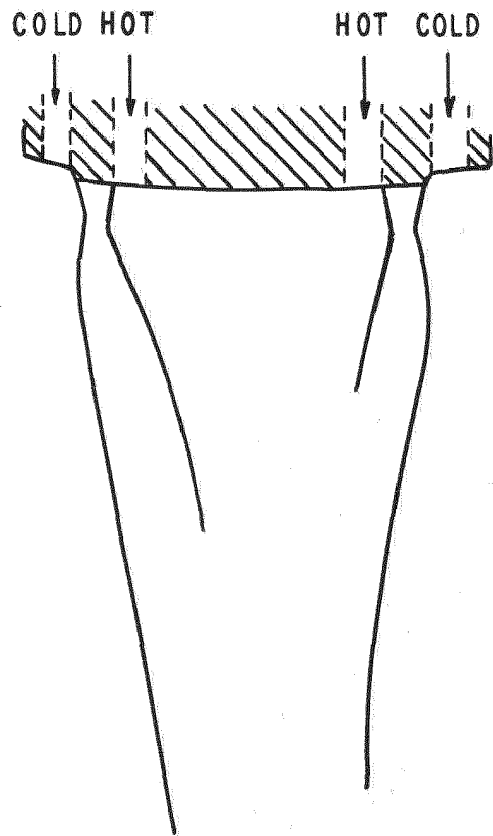




**FIG. 25. PRESSURE DISTRIBUTION ON THE  
GROUND BOARD, C/C RUN.**



FREE AIR



SHADOWGRAPH TRACE

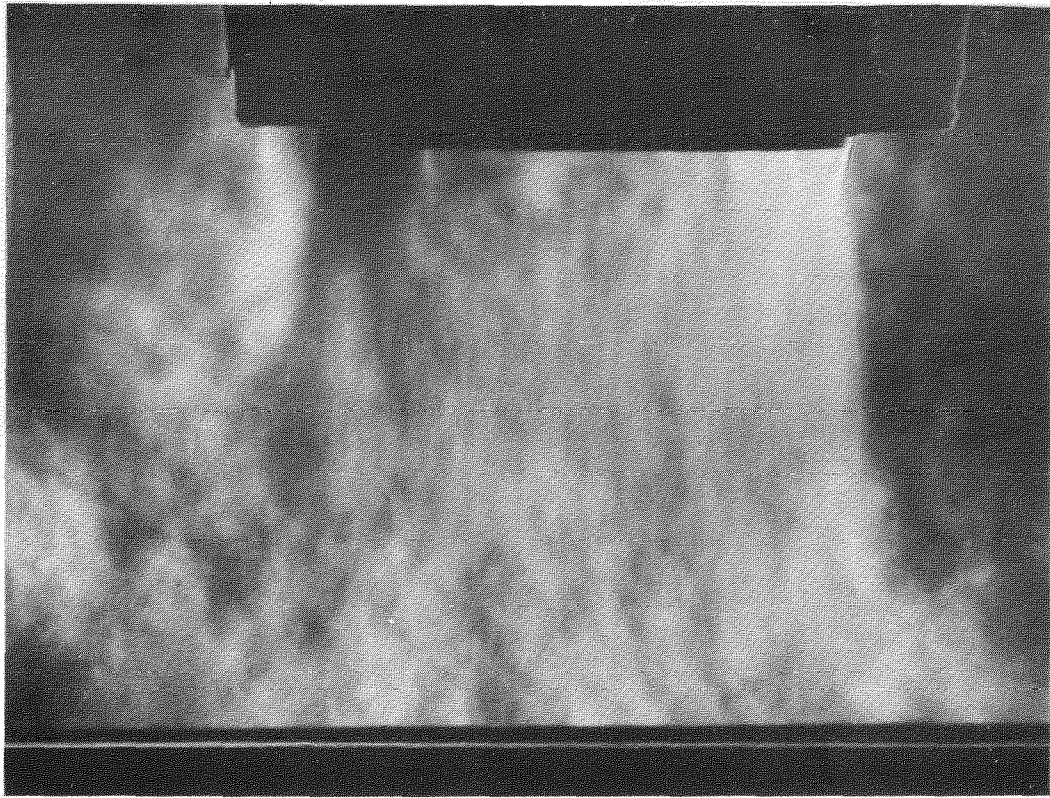
FREE AIR



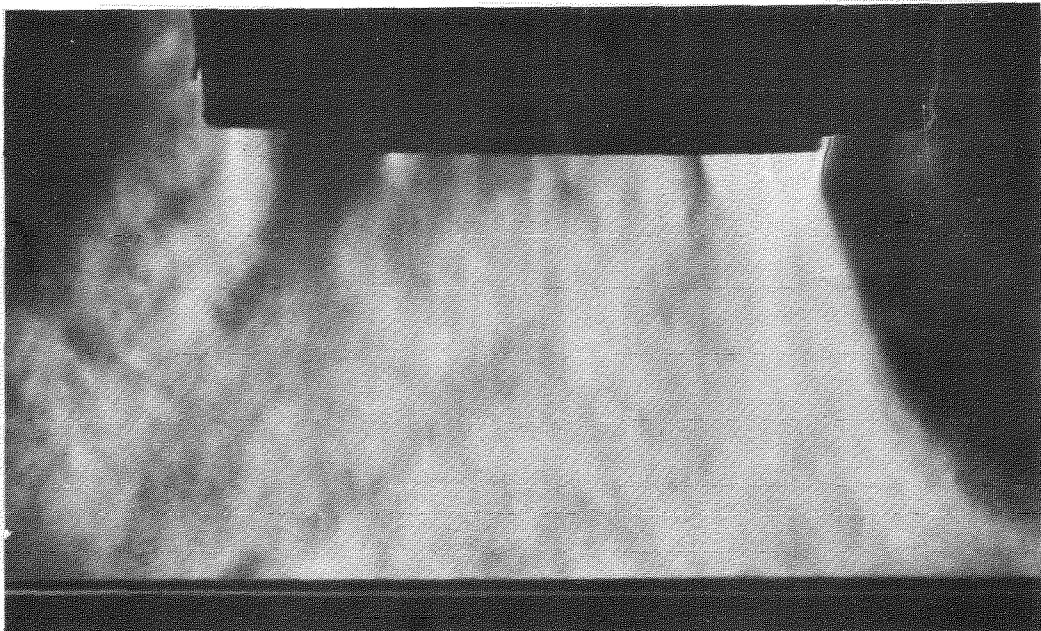
$\frac{H}{D}$

SCHLIEREN PHOTOGRAPHS AND SHADOWGRAPH OF THE

FIG. 27



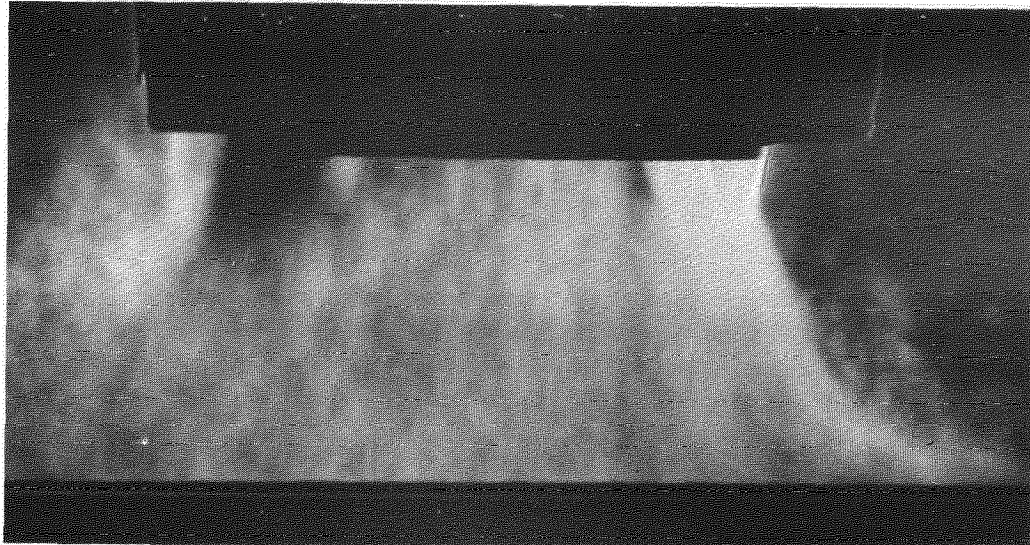
$$\frac{H}{D} = 1.0$$



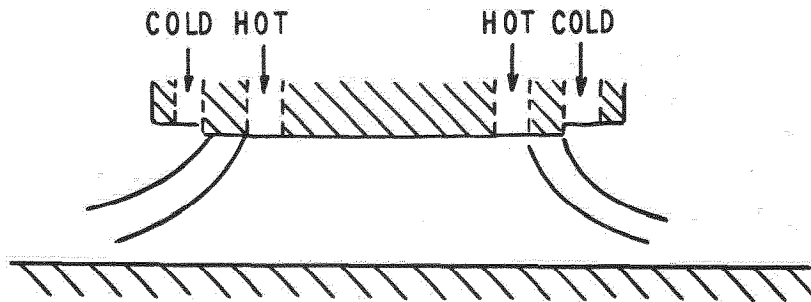
$$\frac{H}{D} = 0.75$$

SCHLIEREN PHOTOGRAPHS OF THE  
FLOW. H/C RUN.

FIG.28

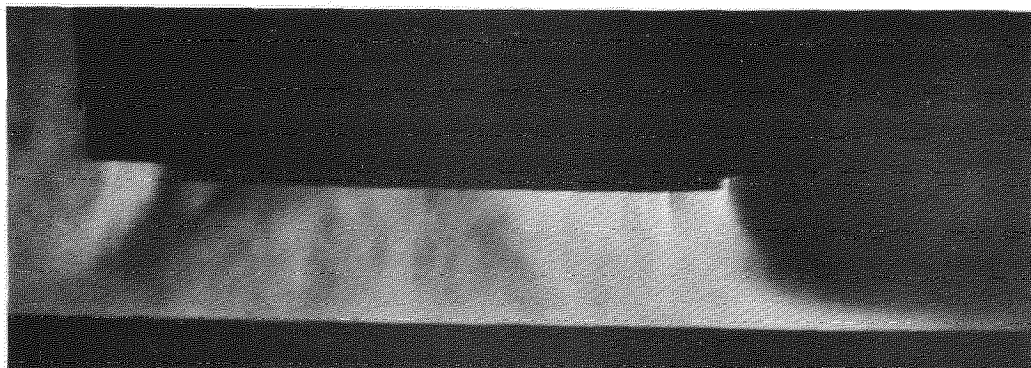


$$\frac{H}{D} = 0.5$$



SHADOWGRAPH TRACE

$$\frac{H}{D} = 0.375$$



$$\frac{H}{D} = 0.25$$

SCHLIEREN PHOTOGRAPHS AND SHADOWGRAPH  
OF THE FLOW. H/C RUN.

FIG. 29.

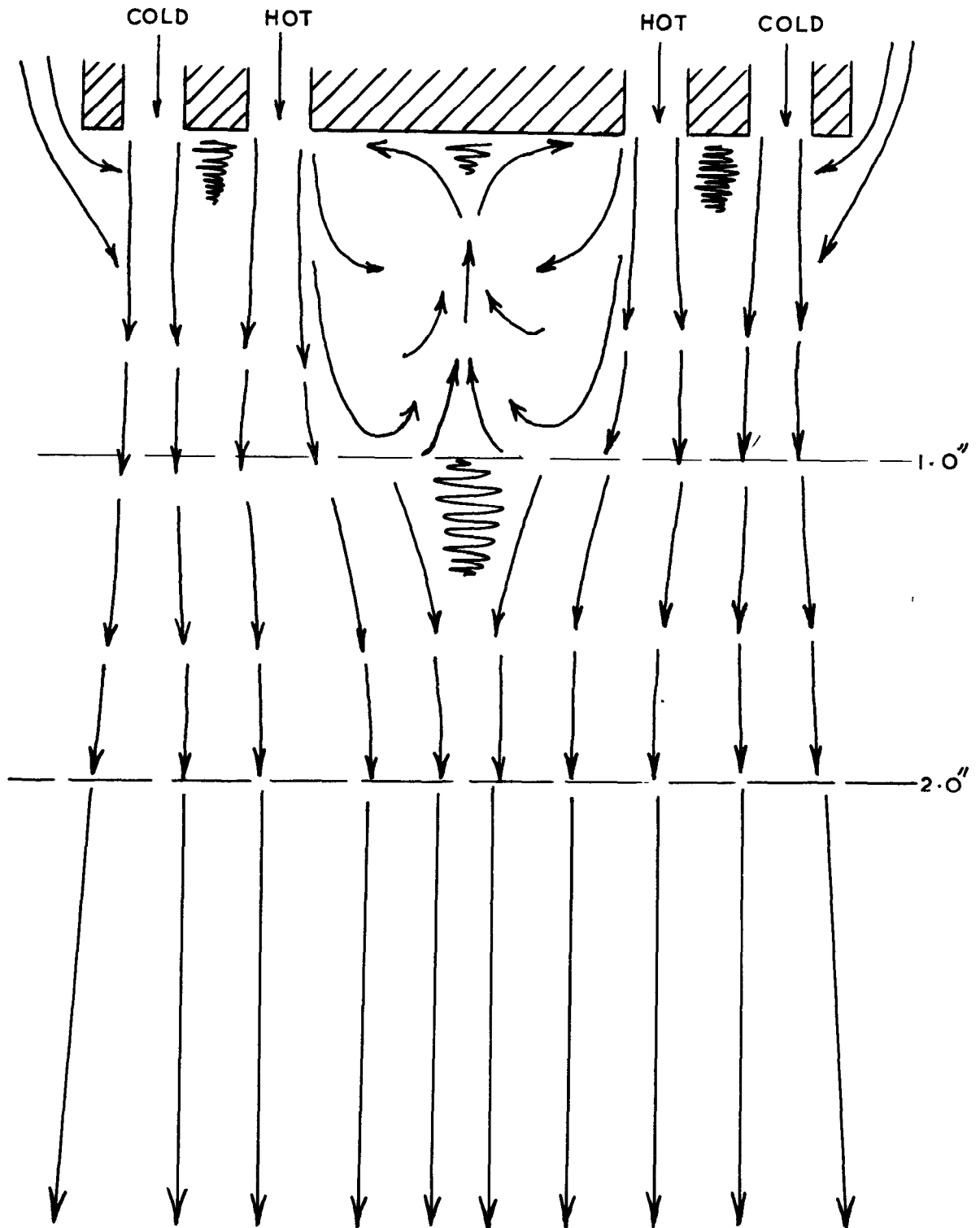
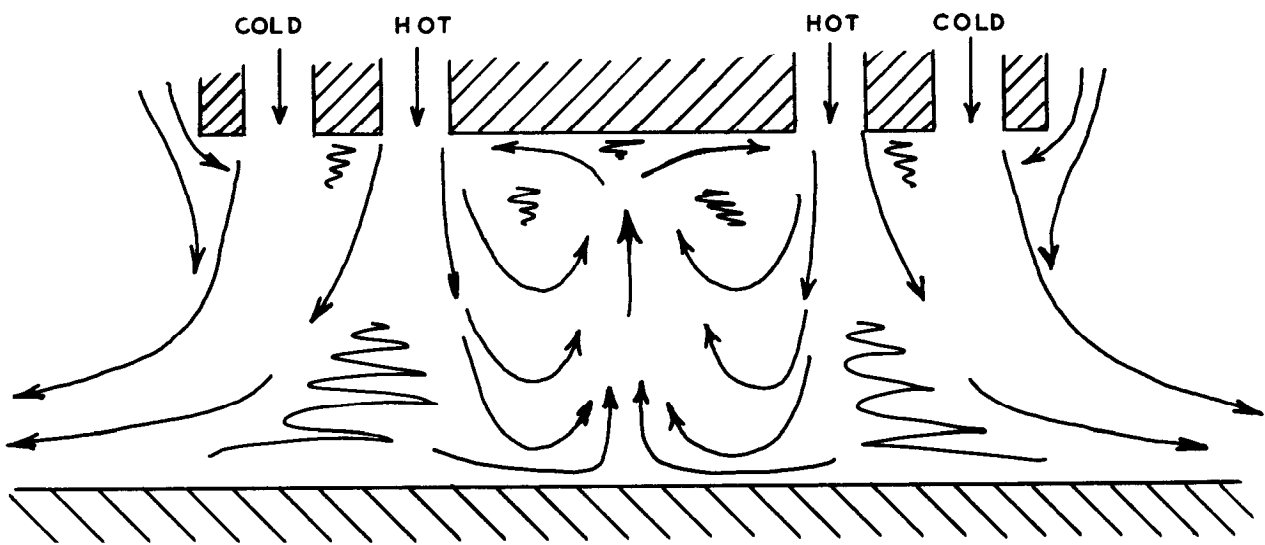
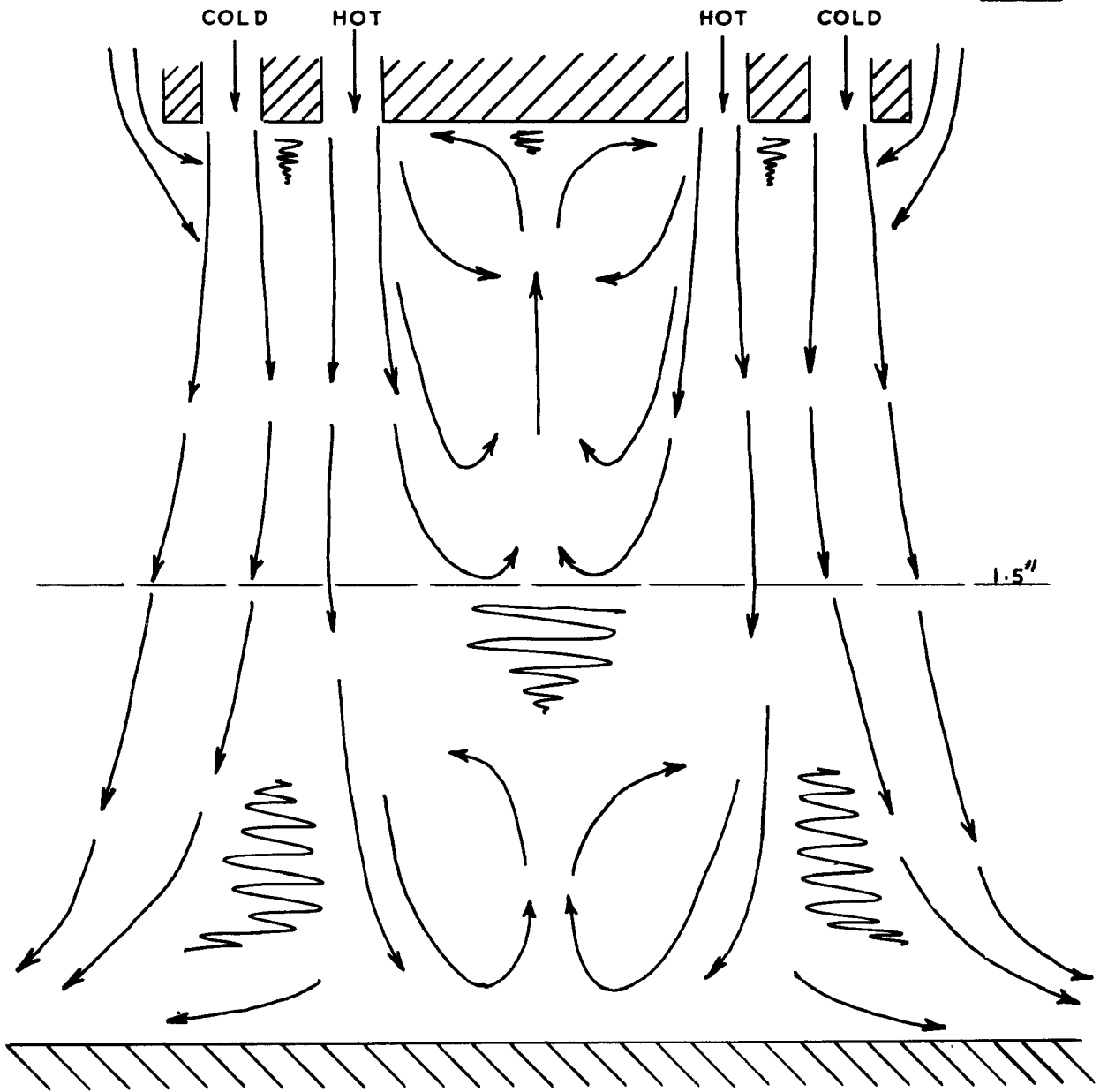


FIG. 29. FLOW INDICATED BY WOOL TUFT  
PROBE. JET IN FREE AIR.

FIG. 30.



© *Crown copyright* 1962

Printed and published by  
**HER MAJESTY'S STATIONERY OFFICE**

To be purchased from  
York House, Kingsway, London, w.c.2  
423 Oxford Street, London w.1  
13A Castle Street, Edinburgh 2  
109 St. Mary Street, Cardiff  
39 King Street, Manchester 2  
50 Fairfax Street, Bristol 1  
35 Smallbrook, Ringway, Birmingham 5  
80 Chichester Street, Belfast 1  
or through any bookseller

*Printed in England*